BIOLOGICS

Combined transcriptomic and proteomic analysis reveals a diversity of venom-related and toxin-like peptides expressed in the mat anemone *Zoanthus natalensis* (Cnidaria, Hexacorallia)

Qiwen Liao[1] · Guiyi Gong[1] · Terence C. W. Poon[2] · Irene L. Ang[2] · Kate M. K. Lei[2] · Shirley Weng In Siu[3] · Clarence Tsun Ting Wong[4] · Gandhi Rádis-Baptista[5] · Simon Ming-Yuen Lee[1]

Abstract

Venoms from marine animals have been recognized as a new emerging source of peptide-based therapeutics. Several peptide toxins from sea anemone have been investigated as therapeutic leads or pharmacological tools. Venom complexity should be further highlighted using combined strategies of large-scale sequencing and data analysis which integrated transcriptomics and proteomics to elucidate new proteins or peptides to be compared among species. In this work, transcriptomic and proteomic analyses were combined to identify six groups of expressed peptide toxins in *Zoanthus natalensis*. These include neurotoxin, hemostatic and hemorrhagic toxin, protease inhibitor, mixed function enzymes, venom auxiliary proteins, allergen peptides, and peptides related to the innate immunity. Molecular docking analysis indicated that one expressed *Zoanthus* Kunitz-like peptide, ZoaKuz1, could be a voltage-gated potassium channels blocker and, hence, it was selected for functional studies. Functional bioassays revealed that ZoaKuz1 has an intrinsic neuroprotective activity in zebrafish model of Parkinson's disease. Since pharmacological blockade of K_V channels is known to induce neuroprotective effects, ZoaKuz1 holds the potential to be developed in a therapeutic tool to control neural dysfunction by slowing or even halting neurodegeneration mediated by ion-channel hyperactivity.

✉ Simon Ming-Yuen Lee
simonlee@umac.mo

1 State Key Laboratory of Quality Research in Chinese Medicine and Institute of Chinese Medical Sciences, University of Macau, Macau, China

2 Pilot Laboratory and Proteomics Core, Faculty of Health Sciences, University of Macau, Macau, China

3 Department of Computer and Information Science, Faculty of Science and Technology, University of Macau, Macau, China

4 Department of Chemistry, The Chinese University of Hong Kong, Shatin, Hong Kong, China

5 Laboratory of Biochemistry and Biotechnology, Institute for Marine Sciences, Federal University of Ceará, Fortaleza, Brazil

Introduction

Zoantharians (Cnidaria: Anthozoa: Hexacorallia: Zoantharia) are an order or marine animals found in shallow tropical and subtropical waters of the Atlantic and Indo-Pacific oceans, which the most common genera are *Zoanthus* and *Palythoa* (Cruz et al. 2016; Reimer et al. 2014). As a genera of Cnidaria, they are the oldest extant order of venomous animals with molecular and fossil data identifying their origin prior to the Ediacaran period ~ 750 million years ago (Erwin et al. 2011; Park et al. 2012). Unlike other venomous animals, Cnidaria lack a centralized venom gland (Macrander et al. 2015). As sister members to sea anemone, they are characterized by penetrant nematocysts, observed in fossils from the Middle Cambrian period, approximately 505 million years ago (Young and Hagadorn 2010), which store complex cocktail of bioactive compounds and peptide/protein toxins and then discharge and inject the venom when capturing prey, and repelling and deterring predators and competitors (Prentis et al. 2018).

Currently, anemone toxins can be categorized into 15 known families as the 4 most common peptide toxins are actinoporin; sea anemone sodium channel inhibitory toxin (type I); sea anemone type II potassium channel toxin; sea anemone type III (BDS) potassium channel toxin and venom Kunitz toxin (Prentis et al. 2018). While many families of sea anemone toxins have been described, little is known about venom components and toxin contents of zoantharians other than sea anemones or jellyfish (Lazcano-Perez et al. 2018). The neurotoxins in Cnidaria venoms are used to paralyze the prey through affecting ion channels and receptors with high selectivity and potency (Ozbek et al. 2009; Rachamim et al. 2015). For instance, it is known that neurotoxins isolated from sea anemones can affect a variety of targets in the central nervous system such as voltage-gated sodium (Na_V) and potassium channels (K_V), acid-sensing ion channels (ASIC), and transient receptor potential vanilloid 1 (TRPV1) (Lazcano-Perez et al. 2016).

Venoms from marine animals have been recognized as an emerging source of peptide-based therapeutics like analgesics, anti-cancer drugs, and drugs for neurological disorders (Peigneur and Tytgat 2018). Several peptide toxins from sea anemone have been investigated as therapeutic leads or pharmacological tools, such as the sodium channel toxins anthopleurin-A and -B that display beneficial effects to be used for cardiovascular disease (Reimer et al. 1985). The peptide APETx2, originated from *Anthopleura elegantissima*, has been implicated in anti-pain effect in inflamed or ischemic tissues with acidosis through inhibiting ASIC3 channel (Diochot et al. 2004; Jensen et al. 2014). Its homologous APETx4 was shown to be active on $K_V10.1$, a potential anti-cancer target (Moreels et al. 2017). Notably, ShK, a potent blocker of $K_V1.3$, as well as its analogs, had already been proved efficacy in animal models of human autoimmune diseases like multiple sclerosis and rheumatoid arthritis (Beeton et al. 2001, 2006). More importantly, ShK-186, which is known as dalazatide, completed Phase 1a and 1b trials recently (Tarcha et al. 2017).

In the manually curated ToxProt database that is composed by 243 toxins from sea anemones (Actiniaria) and 11 toxins from stony corals (Scleractinia), there are only 254 peptide or protein toxins of Hexacorallia (Jungo et al. 2012; UniProt Consortium 2018). This indicates that the already curated Cnidaria peptide toxins show a strong taxonomic bias. Thus, we need to examine the venom peptide profiles from other members of Cnidaria.

Venom complexity should be further confirmed using novel strategies of large-scale sequencing which integrated transcriptomics and peptidomics/proteomics to provide new putative proteins or peptides to be compared among species (Weston et al. 2012; Zhao et al. 2018). There are examples of combination of proteomic and transcriptomic approaches to study venoms of hydra, sea anemones, and jellyfish,

resulting in the discovery of new types of toxins (Balasubramanian et al. 2012; Li et al. 2016; Madio et al. 2017). In consonance with this, we have reported the peptide toxins composition of zoantharians *Protopalythoa variabilis* and *Palythoa caribaeorum* through transcriptomic sequencing previously (Huang et al. 2016; Liao et al. 2018b). However, an integrated proteomic/transcriptomic approach has not been utilized to corroborate the composition of zoantharian cocktail of peptide toxins. In the present study, combination of proteomic and transcriptomic was carried out to describe the peptide toxins composition of the zoanthid *Zoanthus natalensis*—a mat anemone species endemic to Indo-Pacific oceans. This is the first combined analysis of peptide toxin compositions of a zoanthid based on RNA deep sequencing (RNA-seq) data and mass spectrometry (MS) data sets, revealing distinct families of expressed venom-related and toxin polypeptides and highlighting the robustness of using a combined transcriptomic and proteomic approaches to elucidate the peptide toxin arsenals of zoantharians. Furthermore, in silico analysis including molecular dynamics simulation and docking analysis were carried out to predict the affinity between the interested peptide toxins and targeted ion channels. Finally, functional activity assays were performed to validate the hypothesis of candidate peptide toxins linked to the structural analysis and the bioactivity.

Experimental procedures

Zoanthus specimen and sample processing for transcriptomic and proteomic analysis

The zoanthid colony was obtained from a local aquarist and maintained alive in natural sea water until required. Molecular inspection using mitochondria cytochrome oxidase I (COI) gene, as DNA barcoding (Reimer et al. 2006, 2007), confirms that the zoanthid specimen, in this study, is related to the species *Z. natalensis* (Figure S1). Description of sample processing was like described in one of our previous report with minor modifications (Huang et al. 2016). Briefly, several polyps from the single colony were washed in distilled water, chopped with scissors, and dipped immediately into ten volumes of RNAlater (Life Technologies, USA) for RNA preservation. The samples were stored at −80 °C following by storage at 4 °C for 12 h until processing. The minced tissue was powdered by adding five volumes of 2% cetyltrimethylammonium bromide (CTAB) under liquid nitrogen, and then, total RNA was extracted using TRIzol reagent (Ambion, Life Technologies, Carlsbad, California, USA) following the manufacturer's protocol.

For protein extraction, fresh polyps of *Z. natalensis* sample were grinded with a porcelain mortar and pestle under cold RIPA lysis buffer (Beyotime, China). The supernatant

was mixed with 5×cold acetone, 10% (v/v) TCA, and centrifuged after incubation at −20 °C for 2 h. The precipitate was then sonicated in cold lysis buffer. To reduce disulfide bonds and block cysteine residues in the pool of proteins, followed by the addition of 10 mM dithiothreitol (DTT) into the supernatant post-centrifugation. The supernatant was mixed with 5×cold acetone and kept at −20 °C for 2 h. The sample was again centrifuged, and the precipitate collected and freeze-dried. Finally, the lyophilized protein was stored at −80 °C for further proteomic analysis.

Preparation of RNA library and transcriptomic sequencing

The cDNA library was constructed through a standard protocol established by the Beijing Genomic Institute, BGI (Shenzhen, China). Initially, polyadenylated RNA sequences were isolated using oligo (dT). Single-stranded 5′ RNA adaptors were ligated to mRNA fragments using T4 RNA ligase (Ambion, Austin, TX, USA) and then reversely transcribed into cDNA using Superscript III reverse transcriptase (Invitrogen, Carlsbad, CA, USA). 3′ DNA adaptor was ligated to the digested DNA fragments after digestion with *Mme*I, and the products were amplified using PCR. Finally, 100 bp pairend (PE100) RNA-seq was performed on a BGISEQ-500 sequencing platform at the BGI (Shenzhen, China).

Transcriptome analysis

The assembly and assessment of the *Z. natalensis* transcriptome were like described in our previously studies (Huang et al. 2016; Liao et al. 2018a). Briefly, the raw reads were processed to obtain clean reads by removing the adapter sequences and low-quality sequences (i.e., reads in which more than 50% of the bases had quality values ≤ 5) by an in-house C++ script. Raw reads and clean reads were subjected to FastQC: a quality control tool for high-throughput sequence data (FastQC 2011) to evaluate sequence quality. Next, de novo transcriptome assembly was carried out using the short-read assembly program Trinity (version 2.0.6) (Haas et al. 2013). The program combined reads with certain lengths of overlap and connected paired-end reads to form contigs. The TIGR Gene Indices Clustering Tools (TGICL) software (Pertea et al. 2003) was used to obtain the non-redundant unigenes from each sample by splicing and removing redundant sequences.

All reads were realigned to the assembled transcripts using Burrows–Wheeler Aligner (BWA) (version 0.7.7-r441) (Li and Durbin 2010). SAMtools (version 0.1.19-44428cd) (Li et al. 2009) and BEDTools (version 2.17.0) (Quinlan and Hall 2010) were used to evaluate the depth and coverage of the alignment to make sure that both the mapping rate and coverage are higher than 80% thus retained for downstream analysis.

The unigenes from de novo assembly were annotated using BLASTX based on identity with entries from the functionally databases including the NCBI non-redundant protein sequences (nr), UniprotKB/Swiss-Prot, the Kyoto Encyclopedia of Genes and Genomes (KEGG), and the Cluster of Orthologous Groups (COG) databases. In these searches, the BLASTX cut-off was set to 1e−6. The Gene Ontology (GO) annotation was performed using Blast2GO software suite v2.5.0. In the GO mapping process, validated settings were used with a threshold of 1e−6, an annotation cut-off of "55", and a GO weight of "5". Each annotated sequence was assigned to detailed GO terms. The toxin-like and venom-related peptides were predicted by means of BLASTX tools against ToxProt database with the E value of 1e−5. The best matches were selected to predict ORFs using TransDecoder v2.0.1 tool. The predicted proteome was blast against PFAM database to identify functional domains. On the bases of the functional annotation, the peptides were classified into different toxin categories by an in-house Perl script.

Liquid chromatography–tandem mass spectrometry (LC–MS/MS) analysis

The lyophilized proteins were dissolved in fresh prepared resuspension buffer (20 mM Tris–HCl, pH 6.8, 2% SDS, 100 M DTT) and then centrifuged at 14,000 rpm to spin down the undissolved precipitates. The RC DC™ Protein Assay (Bio-Rad, USA) was used to measure the protein concentration and certify that it was higher than 0.5 μg/μl. Filter-aided sample preparation (FASP), a method that combines the advantages of in-gel and in-solution digestion for mass spectrometry (MS)-base proteomics (Wisniewski and Mann 2012; Wisniewski et al. 2009), was utilized for tryptic digestion. After digestion, the liberated peptides were collected by centrifugation.

Liquid chromatography separation was performed by EASY-Spray columns (PepMap® RSLC, C18, 100 Å, 2-μm-bead-packed 50-cm column) (Thermo Fisher Scientific) connected to an Easy-nLC 1000 pump. In each single LC–MS run, a total of 2 μg of tryptic-digested peptides preparation were loaded into the column with buffer A (100% water, 0.1% formic acid) and eluted with a 300-min gradient time, with 5% to 35% buffer B (100% acetonitrile, 0.1% formic acid) at a flow rate of 250 nl/min. Each of the gradients was followed by 1 h of column washing.

Mass spectra were acquired with an Orbitrap Q Exactive mass spectrometer (Thermo Fisher Scientific) in a datadependent manner, with automatic switching between MS and MS/MS scans using a top-10 method (Michalski et al. 2011). MS spectra were acquired at a resolution of 70,000 with a target value of 3×10^6 ions or a maximum integration

time of 200 ms. The scan range was limited from 300 to 2000 *m/z*. Peptide fragmentation was performed via higher energy collision dissociation (HCD) with the energy set at 27 NCE. Charge exclusion was set $z = 1$, 6–8, and > 8 ions. The MS/MS spectra were acquired at a resolution of 17,500 with a target value of 1×10^5 ions or a maximum integration time of 120 ms. The isolation window was 2.0 *m/z*.

Proteomic data analysis

PEAKS Studio (version 8.5) was utilized for peptide and protein identification from the raw data acquired from LC–MS/MS (Zhang et al. 2012a). An in-house proteome database was generated using translated contig sequences from the de novo assembly transcriptome where X represented a gap in the sequences. The MS/MS database search was performed with a 10-ppm mass tolerance for precursor ions and a 0.05-Da mass tolerance for fragmented peptide ions. Cysteine carbamidomethylation was selected as a fixed modification, and N-acetylation of protein, deamidation of asparagine/glutamine, and oxidation of methionine were selected as variable modifications. Trypsin was selected as the protease, with up to two missed cleavages allowed. Results were filtered by a 1% global false discovery rate (FDR). File conversion of mass spectrometry data complied with the instructions in PRIDE (Deutsch et al. 2017; Perez-Riverol et al. 2016; Vizcaino et al. 2014, 2016).

Phylogenetic analysis, molecular dynamics (MD) simulation, and docking analysis

The methodologies to proceed structural protein and dock analysis have been described in our previous works (Liao et al. 2018a, b). Briefly, the phylogenetic comparison of predicted peptide sequences was performed using the program MEGA version 6 with the MUSCLE algorithm as the multiple alignment method (Edgar 2004; Tamura et al. 2013). Reliability of the tree was assessed by the bootstrap method and the node support was determined using 500 bootstrap replicates. Structures of the candidate peptide toxins and U-actitoxin-Avd3i were modeled using SWISS-MODEL server (Arnold et al. 2006). The models were processed in terms of energy minimization and MD simulations with CHARMM27 all-atom force field using the GROMACS 5.1 (Pronk et al. 2013; Van Der Spoel et al. 2005). Each system was subjected to energy minimization of 5×10^7 steps, equilibration in 310 K for 1 ns, and production run for 10 ns, with 2 fs step and van der Waals interaction cut-off at 1.2 nm. Particle-meshed Ewald was employed for the long-range electrostatics; 310 thermostat and 1.0 barostat were used to generate the NPT ensemble. The equilibrated structures were compared to Kunitz-like peptide derived from scorpion (LmKTT-1a) and sea anemone (U-actitoxin-Avd3i),

of which the ZoaKuz1 was considered to be homologous. The PDB ID of LmKTT-1a is 2M01. Structure alignment between ZoaKuz1 and LmKTT-1a (2M01) was performed in PyMOL program (version 1.8, Schrödinger, LLC). After that, since the structure of U-actitoxin-Avd3i has not been validated by experimental procedures, the structure of this peptide was modeled by SWISS-MODEL as mentioned above, using Textilinin (3D65) as template. Molecular visualization and structure alignment were achieved using the PyMOL program (version 1.8, Schrödinger, LLC). The cDNA sequences of the candidate Kunitz-like peptides are shown in table S1.

The atomic coordinates of the potassium voltage-gated channel subfamily A channels including member 1 (UniProt ID: Q09470, $K_V1.1$) were modeled and refined like in our previous study (Liao et al. 2018b). According to the annotations from Uniprot database, S4–S6 domains of the modeled and refined $K_V1.1$ were retained for docking prediction. The fast Fourier transform (FFT)-based, initial-stage rigid-body molecular docking algorithm ZDOCK (Chen et al. 2003a; Pierce et al. 2011) was applied to model the interactions between *Z. natalensis* Kunitz-like peptide and $K_V1.1$ and $K_V1.2$ ion channels. Molecular visualization was achieved using VMD program v1.9.2 (Humphrey et al. 1996).

Peptide synthesis and peptide oxidative folding

The peptides were synthesized by solid-phase chemistry and obtained at a purity grade over 90%, like confirmed by the presence of a single peak in analytical reverse-phase HPLC (RP-HPLC) and electrospray ionization mass spectrometry (ESI–MS) analysis (GL Biochem, Shanghai, China). Complete deprotection and cleavage was carried out essentially with trifluoroacetic acid in water. The crude peptides were precipitated out by the addition of chilled ether. Then, the crude peptide was purified by HPLC, freeze-drying, and retested by HPLC to make sure that it was qualified (Figure S2).

Oxidative folding was performed as follows: peptide was dissolved to a final concentration of 80 μM in degassed 300 mM Tris–HCl buffer (pH 8.5). Then, 1 mM glutathione disulfide (GSSG) and 10 mM glutathione (GSH) was added to the solution. Nitrogen gas was bubbled into the solution to protect the peptide and avoid unwanted air oxidation. The folding reaction was allowed to occur for 96 h and monitored by analytical HPLC and MALDI-TOF. Afterward, the peptide folding reaction was quenched by acidification, followed by lyophilization. The samples were then purified by preparative reverse-phase HPLC. The peptide fold conversion was calculated by the own HPLC system (Waters), reaching the rate of 55%, and the isolated yield calculated to be 26%. The peptides were solubilized in Milli-Q water to make a

1 mM stock solution and stored at $-20\,^{\circ}$C until required for functional assays.

Zebrafish maintenance

Wild-type zebrafish was manipulated as described in the Zebrafish Handbook (Westerfield 2000). Briefly, the zebrafish was maintained in standard conditions at 28 °C with a 14 h/10 h light/dark cycle. The zebrafish was fed twice a day with brine shrimp and general tropical fish food. The embryos were generated by natural pairwise mating (3–12 months old) and raised at 28.5 °C in embryo medium. The ethical approval for the animal experiments was granted by the Animal Research Ethics Committee from the University of Macau.

Anti-tyrosine hydroxylase (TH) whole-mount immunostaining

Anti-tyrosine hydroxylase (TH) whole-mount immunostaining of zebrafish was carried out as previously described (Zhang et al. 2012b). Briefly, zebrafish embryos at 1-day post-fertilization (dpf) were exposed to 250 µM 6-hydroxydopamine (6-OHDA) with or without the peptides for 2 days. Then, the zebrafish larvae were fixed with 4% paraformaldehyde in PBS for 30 min, rinsed, and stored at $-20\,^{\circ}$C in absolute methanol. Semi-quantification of TH$^+$ cells was assessed by an investigator blinded to the drug treatment history of zebrafish, using ImageJ software (Schneider et al. 2012). Results were expressed as fold changes of area of TH$^+$ cells in control group.

Locomotion behavioral test

The locomotion test was carried out as described in our previous study (Zhang et al. 2012b). Briefly, the wild-type strain zebrafish larvae at 3 dpf were under co-treatment of 250 µM 6-OHDA with various concentrations of the peptides for 4 days. Zebrafish at 7 dpf were transferred into 96-well plates (1 fish/well). The 96-well plates were put into a Zebrabox and the swimming behavior was monitored by an automated video tracking system (Viewpoint, ZebraLab, LifeSciences, Lyon, France). Before the start of data acquisition, the larvae were settled to accommodate themselves to the environment in the Zebrabox. The swimming pattern of each fish was recorded in five sessions of 10 min each. The total distance traveled was recorded as the distance that a given zebrafish larva was capable of swimming during the 10-min-long session. A statistical analysis of the total distance traveled by each zebrafish larva in the different treatment groups was performed using the one-way ANOVA and Dunnett's test.

Results

Transcriptome sequencing, de novo assembly and assessment

cDNA prepared from whole tissues (polyps) of a single colony of *Z. natalensis* colony was sequenced using BGISEQ-500. After sequencing and cleaning the low-quality reads, we acquired 149,351,954 clean reads. The clean data are available at the National Center for Biotechnology Information (NCBI) Sequence Read Archive (SRA) under accession number SRP154951. Using Trinity program for the de novo assembly, the clean reads were then clustered together using TGICL into consensus transcript sequence, and a total of 225,236 contigs were generated with a mean sequence length of 697 bp (Table 1). The Transcriptome Shotgun Assembly (TSA) project was deposited at DDBJ/EMBL/GenBank under the accession GGTW00000000 associated with the BioProject PRJNA480736. The version described in this paper is the first version, GGTW01000000.

Table 1 Description of de novo assembly and annotation of the transcriptome

Assembly	
Raw reads (pair end)	375,896,776
Clean reads	149,351,954
Number of contigs	225,236
Average length of contig	697.13 bp
Minimum contig	200 bp
Maximum contig	24,409 bp
GC content	44.83%
Transcripts with significant BLAST hit (1×10^{-5})	
With homologs in database	
Acropora digitifera	42,033
Nematostella vectensis	40,091
Hydra vulgaris	33,201
Palythoa caribaeorum	78,871
Protopalythoa variabilis	72,546
Functional annotation	
Nr	69,963
Nt	16,334
Swissprot	40,998
KEGG	43,278
KOG	40,455
GO	11,532
ToxProt	213
Proteomics analysis	
Protein groups	2754
Annotation in ToxProt	162
Peptide toxin presence with transcripts	30

Functional annotation of *Z. natalensis* transcriptome

Diverse public protein databases were applied in this study, including Nr, Nt, Swiss-Prot, KEGG, and euKaryotic Orthologous Groups (KOG). Among the achieved 183,215 unigenes, 69,963 (38.19%), 40,998 (22.38%), 43,278 (12.46%), and 40,455 (22.08%) have matches in the Nr, Swissprot, KEGG, Swiss-Prot, and KOG databases, respectively. In total, there are 78,658 (42.93%) unigenes

functionally annotated on basis of the searched databases (Fig. 1a). In pathway enrichment, the KEGG Ortholog (KO) database categories were assigned to the unigene sequences using the KEGG Automatic Annotation Server (KAAS). In total, 10,028, 11,481, 18,086, and 20,898 unigenes were identified in cellular processes, environmental information processing, metabolism, and organism system, respectively. The top five enriched KEGG pathways were represented by signal transduction, global and overview maps, cancers,
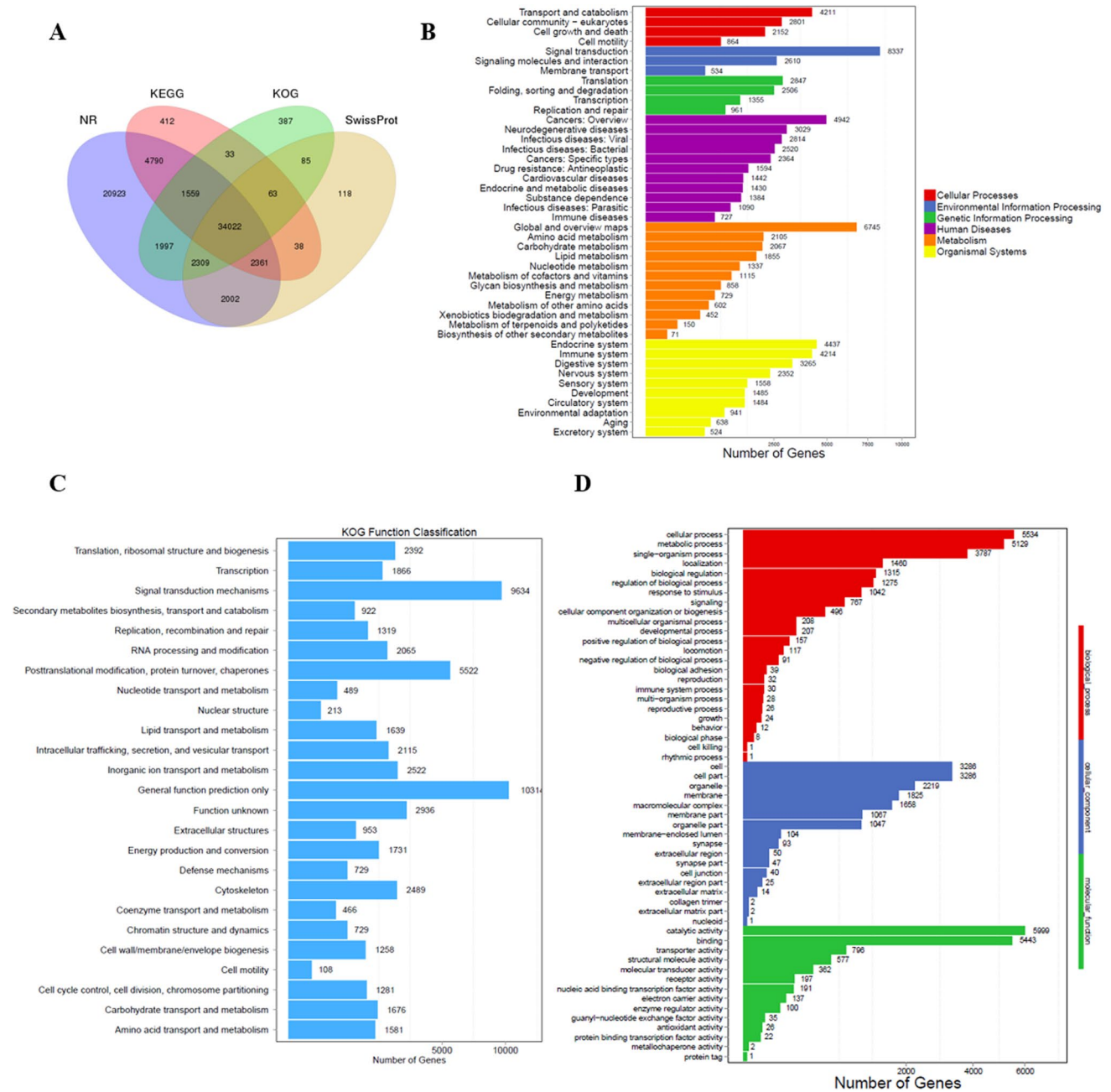
Fig. 1 Functional annotation of *Z. natalensis* assembly. **a** Venn diagram of homologous transcripts from nr databases, KEGG, KOG, SwissProt. **b** Specific significantly enriched KEGG pathways of anno-

tated unigenes. **c** euKaryotic Orthologous Groups (KOG) annotation of putative proteins. **d** Gene Ontology (GO) enrichment of the annotated unigenes

endocrine system, and immune system with 8337, 6745, 4942, 4437, and 4214 hits, respectively. Main organismal system pathways were endocrine system (4437), immune system (4214), and digestive system (3265) (Fig. 1b). The unigenes were aligned to the KOG database to predict and classify their presumed functions. Of the 183,215 unigenes, 40,455 were assigned to 25 clusters. Among the 25 KOG categories, the cluster for general functional prediction (10,314 unigenes, 25.49%) represented the largest group, followed by signal transduction mechanisms (9634 unigenes, 23.81%) and post-translational modification, protein turnover, and chaperones (5522 unigenes, 13.64%). Cell motility (108 unigenes, 0.27%), nuclear structure (213 unigenes, 0.53%), and coenzyme transport and metabolism (466 unigenes, 1.15%) represented the smallest groups (Fig. 1c). GO enrichment analysis was performed to classify gene functions of these unigenes. Unigenes were enriched into 55 GO classes, in which catalytic activity, cellular process, binding, and metabolic process are the top four enriched classes, with 5999, 5534, 5443, and 5129 annotated unigenes, respectively (Fig. 1d).

Shotgun proteomic analysis

From the proteomic analysis, a total of 52,760 MS spectra and 224,543 MS/MS spectra were generated A total of 19,813 peptide sequences and 2745 unique protein regions were identified (Table 1, Fig. 2). The quality was reflected by precursor mass error of PSM and shown in Figure S3. The mass spectrometry proteomic data were deposited in the ProteomeXchange Consortium via the PRIDE partner repository (https://www.ebi.ac.uk/pride/archive/) with the data set identifier PXD010839.

Venom-related polypeptides and peptide toxins identified in *Z. natalensis* transcriptome and proteome

All the unigenes obtained from the transcriptomic analysis were blasted against the Tox-Prot database in the SWISS-PROT. A total of 212 predicted venom-related and toxin-like peptides were classified into seven functional categories based on searching against PFAM database. These include: allergen and innate immunity components, venom auxiliary proteins, mixed function enzymes, membrane-active peptides, protease inhibitors, hemostatic and hemorrhagic toxins, and neurotoxins (Fig. 3). To confirm the presence of these toxins, within these categories expressed in *Z. natalensis*, overlaps of peptide sequences identified independently through proteomic and transcriptomic analysis were obtained by an in-house Perl script. By this means, a total of 162 peptide sequences could be annotated in

ToxProt database with 30 peptide toxins identified in both transcriptomic and proteomic analyses (Table 2). The peptide sequences are shown in Table 3.

Molecular phylogenetic analysis

From the toxin identification, it was noticed that Kunitz-like peptides has an abundant expression and presence in *Z. natalensis* transcriptome and proteome. Thus, transcripts with highest bit-score which are homologous to Kunitz peptides were selected to perform molecular phylogenetic analysis using MUSCLE algorithm and MEGA6 program. As shown in Fig. 4a, Unigene38169 was similar to a bifunctional (both protease inhibitor and neurotoxicity) Kunitz peptide from sea anemone. However, the C-terminal was divergent, lacking an additional alpha–helix and a third disulfide bridge. Predicted *Z. natalensis* Kunitz-like peptides, including the transcripts CL14246, Unigene59550, and Unigene149397, were also different from sea anemone toxins that have Kunitz-domain in their structure. From the phylogenetic tree shown in Fig. 4b, CL14246 could be clustered with Kunitz peptides from snake and spider, being closer with snake type. Interestingly, Unigene59550 and Unigene149397 could be perfectly clustered with scorpion Kunitz peptides, whereas Unigene59550 was closest to homologous sequence from sea anemone.

Structure modeling, MD simulation, and docking analysis

After obtaining the homology models of the candidate peptides, MD simulations were employed to refine the modeling structures. As shown in Fig. 5, the root-mean-squared deviation (rmsd) values after 1 ns simulation of CL14246, Unigene38169, and Unigene 59550 reached a plateau at about 0.1 Å, while Unigene149397 remains at 0.3 Å over the course of simulation. These indicate that structures of all three peptides, obtained from the homology modeling, are quite stable. As Unigene59550 was also present in the proteomic analysis, it was named as ZoaKuz1 and was further studied in functional assays. Again, in the multiple sequence alignment and phylogenetic analysis, it was shown that ZoaKuz1 was homologs of known Kuntiz-like toxins from sea anemone (P0DN10, U-actitoxin-Avd3i) and scorpion (P0DJ46, LmKTT-1a), but clustered with LmKTT-1a, according to the maximum-likelihood tree. Molecular docking analysis was performed on $K_V1.1$ with the peptide ZoaKuz1using ZDOCK and compared with the toxins U-actitoxin-Avd3i and LmKTT-1a, as positive control. In structural alignment, the ZoaKuz1 model matched well with U-actitoxin-Avd3i and LmKTT-1a with rmsd value is 0.907 and 2.098 Å (Fig. 6a,

Table 2 Description of candidate peptide/protein toxins from *Zoanthus natalensis* transcriptome

| Toxin group	Toxin family Pfam domain	Num. of contigs	Presence in proteome	Acc (hmm)	Identity
Neurotoxin					
ShK/aurelin	ShK	3	–	0.64–0.98	23–24%
Scoloptoxin	NA	1	–	NA	27.68%
Turripeptide	kazal	16	2	0.70–0.99	33.93–65.38%
Kunitz-type protease inhibitor	Kunitz_BPTI	11	2	0.50–0.98	37.21–65.45%
Cysteine-rich venom protein	CAP	2	–	0.84–0.89	33.78–35.71%
Alpha-latrocrustotoxin-Lt1a	Ankyrin repeats	3	1	0.59–0.95	21.26–31.93
Perivitellin-2	MACPF	1	1	0.93	22.11%
Hemostatic and hemorrhagic toxin					
Snake venom VEGF toxin	PDGF	3	2	0.6–0.9	23.75–28.78%
C-type lectin	Lectin_C	12	1	0.57–0.96	26.52–37.31%
Ficolin lectin	Fibrinogen_C	28	–	0.53–0.98	27.54–58.93%
Venom prothrombin activator (F5/8 type C)	F5_F8_type_C	59	10	0.55–0.96	22.64–48.94%
Venom prothrombin activator (Peptidase S1)	Trypsin	3	–	0.87	34.38–40.98%
Snake venom peptidase S1	Trypsin	1	–	0.92	41.79%
Venom metalloproteinase M12B/disintegrin	Disintegrin	1	–	0.9	41.27%
Protease inhibitor					
Thyroglobulin type-1 protease inhibitor	Thyroglobulin_1	6	2	0.58–0.91	25.41–60%
Membrane-active peptides					
Waprin	WAP	10	–	0.46–0.98	25.41–59.26%
Mixed function enzymes					
Phospholipase A2	Phospholip_A2_1	6	–	0.84–0.90	38.10–43.22%
Acetylcholinesterase	COesterase	3	–	0.83–0.92	26.87–32.54%
L-Amino-acid oxidase	Amino_oxidase	3	–	0.72–0.76	23.81–24.14%
Venom phosphodiesterase 2	Phosphodiest	9	2	0.86–0.94	29.70–45.16%
Endothelial lipase	PLAT	2	–	0.84	26.36%
Venom auxiliary proteins					
U-actitoxin	IGFBP	1	–	0.88	62.75%
Calglandulin	EF-hand_7	1	–	0.88	33.80%
Neprilysin-1	Peptidase_M13_N	12	5	0.63–0.98	28–34.05%
Metalloprotease toxin	Astacin	1	–	0.88	30.70%
Hyaluronidase	Glyco_hydro_56	3	–	0.84–0.96	37.88–42.86%
Venom protein 302	VWC	1	–	0.92	48.08%
Allergen and innate immunity					
Venom protease	Trypsin	2	–	0.87–0.88	40.68–50%
Serine carboxypeptidase	Peptidase_S10	1	–	0.9	40.43%
Venom allergen	CAP	2	–	0.81–0.86	27.37–30.32%
Venom dipeptidyl peptidase	DPPIV_N	2	2	0.95	31.88–33.07%
Techylectin-like protein	Fibrinogen_C	4	–	0.84–0.93	32.88–45.95%

b). From docking analysis, ZoaKuz1 could block the pore of $K_V1.1$ with Gibbs free energy (ΔG) of -37.5 kcal/mol (Fig. 6c). Hydrogen bonds are formed between Arg29 and Lys45 of ZoaKuz1 and Glu353 and Asp377 of chain D of $K_V1.1$ with distances of 2.55 and 3.20 Å, respectively (Fig. 6d). In case of the positive controls, both known Kunitz peptides, i.e., U-actitoxin-Avd3i and LmKTT-1a, bind to $K_V1.1$ with ΔG of -44.4 and -46.3 kcal/mol

(Fig. 6e, g), with their respective interactive sites shown in Fig. 6f, h, respectively.

Peptide oxidative folding

Oxidative folding was successfully reached, after linear peptide synthesis, in the presence of GSSG/GSH,
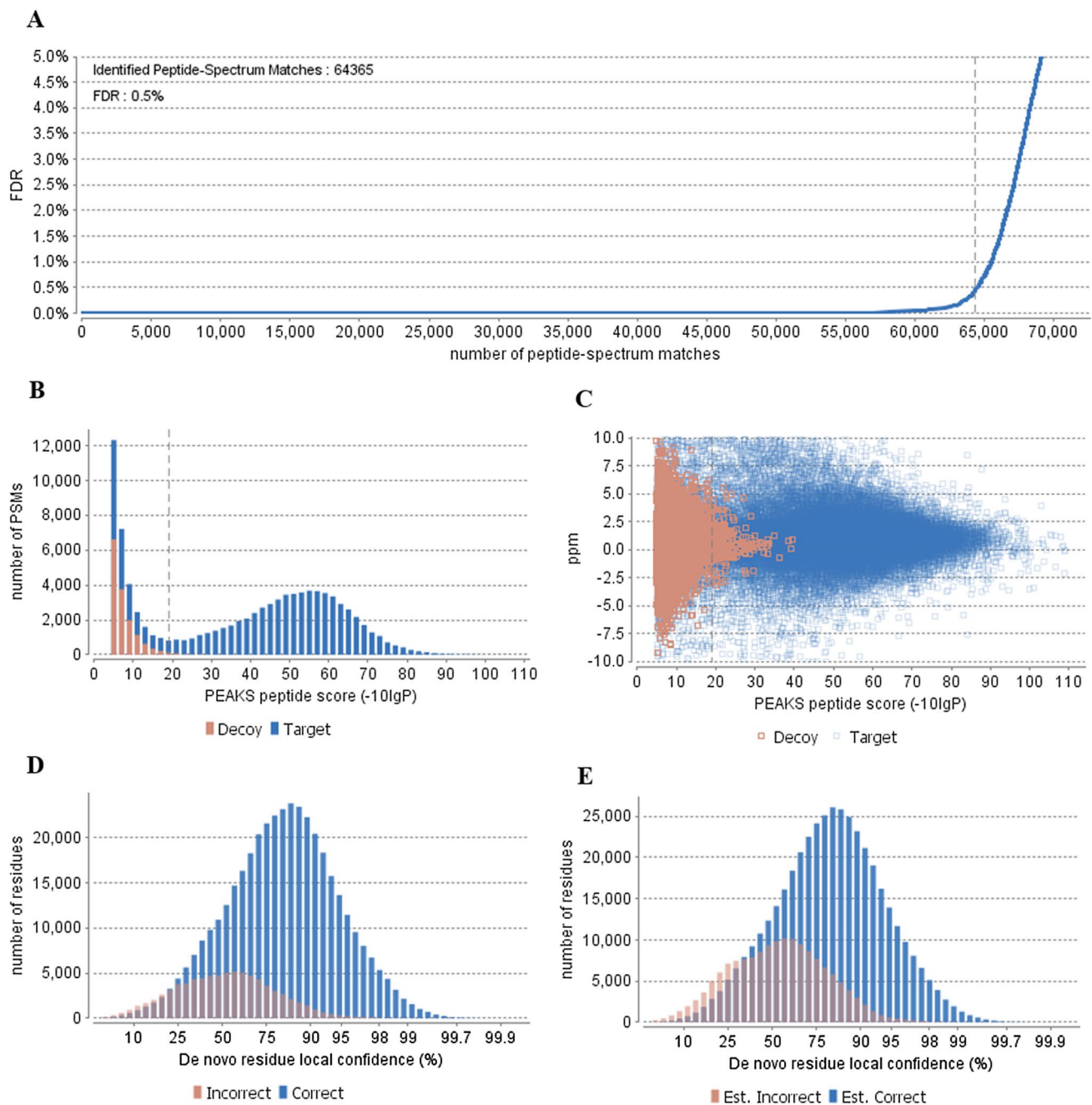
Fig. 2 Statistics of *Z. natalensis* proteomics analysis. **a** FDR curve. *X* axis is the number of PSM being kept. *Y* axis is the corresponding FDR. **b** Distribution of PEAKS peptide score. **c** Scatterplot of PEAKS peptide score versus precursor mass error. Distribution of residue local confidence is shown as: **d** residues in de novo sequences validated by confident database peptide assignment; **e** residues in "de novo only" sequences

with a buffered solution containing a low concentration of ZoaKuz1 (80 μM), in an anoxic atmosphere of nitrogen. After 48 h of oxidative folding process, constantly monitored by RP-HPLC, the disulfide-folded peptide (MW = 6140.610) was formed, like confirmed by MALDI-TOF (Fig. 7).

ZoaKuz1 prevented 6-OHDA-induced DA neuronal loss in zebrafish

To confirm the neuroprotective effect of ZoaKuz1 in vivo, TH staining was used to evaluate the DA neuron system of zebrafish larvae. As shown in Fig. 8, DA neurons were decreased in the diencephalon (indicated by the yellow
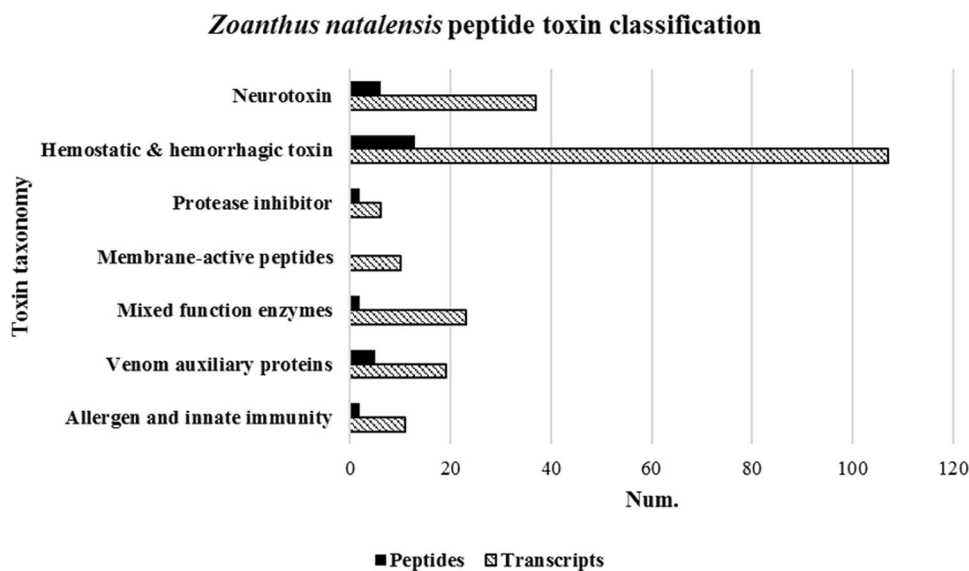
Fig. 3 Classification of putative *Z. natalensis* toxins according to HMM search against PFAM domain database scan. Two categories of toxins, including neurotoxin, hemostatic and hemorrhagic toxins, comprise 107 and 26 peptides each, respectively. These contain the most abundant numbers of all putative peptides. Within neurotoxin, there are six toxin types: ShK/Aurelin, scoloptoxin, turripeptide, cysteine-rich venom protein, latrocrustotoxin, and perivitellin. The third most abundant toxins are mixed function enzymes. The forth most prevalent expressed toxins are peptides related to venom auxiliary proteins. The left two categories are protease inhibitors, membrane-active peptides, and peptides related to allergen and immunity

brackets) of zebrafish larvae after treatment with 6-OHDA. On the other hand, ZoaKuz1 significantly alleviated the loss of DA neurons when zebrafish larvae were exposed to concentration as low as 0.2 μM of ZoaKuz1, indicating that low dose of ZoaKuz1 effectively induces neuroprotective effects against 6-OHDA-induced DA neuron loss in zebrafish larvae.

The 6-OHDA markedly altered the swimming behavior of the zebrafish as a consequence of dopaminergic neurons (Anichtchik et al. 2004). As shown in Fig. 9, the total swimming distances of the zebrafish larvae decreased significantly after exposure to 6-OHDA. When the zebrafish larvae were co-treated with 6-OHDA and ZoaKuz1, 6-OHDA-induced lesion of swimming behavior of the zebrafish larvae was reversed with 0.5 μM ZoaKuz1.

Discussion

Unlike some of the most known and common venomous animals such as snakes, lizards, and cone snails that attract public attention due to not only the repulsive encounters and harmful consequences of contact with these animals, but also in reason of the widely recognized venom-derived developed drugs, such as Captopril®, Byetta®, and Prialt® (King 2011; Robinson et al. 2017), venomous marine animals of other groups than sea anemones and jellyfishes have received comparatively low attention. The potential of cnidarians, like zoanthids, as source in drug discovery

platforms has been underestimated, coincidently as the general public is not aware that they are animals rather than plants (Prentis et al. 2018) and are more than harmless pets to decorate home aquariums. More than a century of research on Cnidaria, especially on sea anemone venoms, has revealed that they abounds in biologically active peptides and proteins, despite more recent omics studies have indicated that much of the venom proteome remains unexplored (Madio et al. 2017). Moreover, there is no doubt that some of these new discovered cnidarian peptide toxins, particularly from non-model organisms, will prove to be effective pharmacological modulators that could be tamed to be developed into therapeutic leads (Prentis et al. 2018). In principle, two approaches can be utilized for venom-based drug discovery: assay-guided fractionation, which was based on pharmacological screening of crude venoms in conjunction with iterative separation and purification steps such as high-performance liquid chromatography (HPLC). Purified venom peptides are sequenced using Edman degradation; or the systematic identification of putative bioactive venom components using proteomic, transcriptomic, genomic, and bioinformatics approaches. Synthetic peptides will then be progressed to detailed pharmacological and activity testing (Oldrati et al. 2016; Prashanth et al. 2017). Assay-guided discovery is usually directly at a specific target, limiting the breadth of bioactivity that is available for discovery (Prashanth et al. 2012). Sequencing the transcriptome of the transcriptome of the venom secreting organ can help

Table 3 Sequences of peptide toxins identified from proteomics analysis

Z. natalensis contigs	Protein sequence	Uniprot match	Pfam domain	Identity (%)
Neurotoxin				
Kunitz toxin				
Unigene59550	VCELPKFTGPCRAAFQRYYFNKKSGKCS RFIYGGCKGNSNNFRTKLECKLKCR	P0DN10	Kunitz_BPTI	62.75
Unigene152864	ETGKSGRLMCKFNGRPETVTWSKDGEA NVGALDHITANGVVMDFSVVKSSDRGVY RCTASDGAGSIAASI	A5X2X1	Kunitz_BPTI	38.46
Turripeptide				
CL20909.Contig1	DPCLVKKCEFHSKCVNRDGGARCVCPSC N	P0DKT1	kazal	55.56
Unigene77303	KANCVCNEICFLIYAPVCASDGNTYASEC VMNVASCKKNITLTIAKREPC	P0DKT1	kazal	42
Alpha-latrocrustotoxin-Lt1a				
Unigene42296	QTDIKNKQNLTPLTLAAKIGQKEMFNHIL NRD	Q9XZC0	Ank	24.49
Perivitellin-2				
Unigene14196	FEFSASASYQKSNSDVASRNYVYVISKAT CTSHFSMLEYSNPPPFSDSFINSAKALASA QATAEDVADFIDNYGTHFLDEVTFGSSYT QQHRMTTTTFESMDTEKYGVAVQAGYSG MISVGGGFGLDSEQRQAASSFSKKVETST VTVGSAPPSNGEAMTWASATKDNPVPIK YRLRPITELFTDEF	P0C8G6	MACPF	22.11
Hemostatic and hemorrhagic toxin				
Venom prothrombin activator				
CL59.Contig2	PTNLVILFDSNCPRVNISWKAPTSPNGVIN HYTVYYRYLPNGNISIVNVMAGIMTVTLD IIGGMKYRFEVTATTVA	Q7SZN0	F5/8 type C	25
CL6358.Contig1	REDSSQWTRVKKTKDAEVLKRKGDNRA PIHKAYINLEDVPYSEAVDLINNWNTRPK WDETFAVVHVLDDVDNFKVLYMCIKTPP LFRRREIVLATKEKEDKGEHEVPFHIVAW RSTKHPSVAEPDTALKKPSLIRVQALTSGI IIRPVDDGAQSSKLVVITQL	Q58L91	F5/8 type C	32.69
CL6453.Contig1	MDAWCSPVSDENQFIQFDMGEKTKVTRI ATQGDPASGGKFVKSYVMLYSNNGKKF DVYNEDGKKEKVFEGNADIFNVKHNNL KKPVVARYLRINPRTWDKGICLRTEL	Q7SZN0	F5/8 type C	32.28
CL20605.Contig2	FSASSYHSNTYLPHFARLNGSKYWTTTRD GRDKAWLQIDLGNVYTICAIETQGSAIMIF REWSKEYLVTLSTNGDSWTPYKE	Q7SZN0	F5/8 type C	37.27
Unigene510	ASTGTGSNGRLYNTGSAWCGTTPPSDYL QVDLGQSVTVTG	Q58L90	F5/8 type C	30.74
Unigene11574	IRAYSEYNSNYIAADGRLHYNPHNKHYH GWLPSASDVHQWLGVTFKKWTQINYIQT QGRENAGQWVSSYILKYSYDGVDYVSYK QNGRTGVFLGNSNNNGVHGNPIDPPIIAR AIRIV	Q58L91	F5/8 type C	28.66
Unigene34275	NVETVDSCFTKASLDHYKMFFMKNQNE CWAAD	Q58L91	F5/8 type C	44.44
Unigene73653	CAESNGGCSHNCSEPKPGIVVCQCPLGY KLLSLGKIC	Q7SZN0	F5/8 type C	28.4
Unigene90060	LKASSQYNVNFKPGNGRLHLHAYQVS GNGAWSPSSSSKMQWLQVNFGKAAK ITRIATQGRQDGNWYVTKYSLSYSYDG VFFEDYQV	Q7SZN0	F5/8 type C	32.59

Table 3 (continued)

| *Z. natalensis* contigs	Protein sequence	Uniprot match	Pfam domain	Identity (%)
Unigene143484	KVTKVATQGRPGVIQWVKTYTLWYSNN GISFLPYKVNGRTKVFDGNQNWNVIKTN VIDPPIIARSIRIQVESYHSFVALRIEF	Q593B6	F5/8 type C	35.83
Vascular endothelial growth factor				
Unigene25734	HHCNPKTMSYDQDICQCICKEDGSSC	P83906	PDGF	28.78
Unigene26067	CSCECRDTNPKCNDTFQRWNDQT	C0K3N4	PDGF	24.58
C-type lectin lectoxin				
CL431.Contig1	KKTFSAAKADCESQNAHLITIPNTWEEEQ FWIRQVQEDLPINNDKAQDFSTVPGLPQ WYVWIGMRYNSELDMFEWENGTPA	A7X409	Lectin C-type domain	27.62
Protease inhibitor				
U24-ctenitoxin				
Unigene160034	PPPPGMYVPQCKTDG	P84032	Thyroglobulin_1	25.41
Unigene161096	YEQSIKNHVLGRWIPRCRLDGSYDPVQ CDRGWSCWCVDD	P84033	Thyroglobulin_1	32.29
Mixed function enzymes				
Venom phosphodiesterase				
CL6618.Contig3	CVSHHSMLTGLYVESHGMVGNSFWDPV YQQEFHIAYDCTNYDKKFWNASEPVWLT LQKNGGHSGMFIWPGYNGYPEKPTYYE KPVCNINCSSVYSWVPPSAINYNCISNLS VPLRSRIDKVMSWLTSKVNPPTFVAMQF GDADLQGHNHGPISPQYKEGVEQFDRDI VGYFMSSLRNSGLENETNVIFVSDHSFVE TSSSRQFYLSDYLDSDSYHGLVETTLAHII PKAGKEEEIYKNLTANKHPNITIYRKNEI PDIFHWKNNRRIPPIFLLADLGWVITKER PSLSKNWTKGTHGYS	J3SEZ3	Phosphodiest	32.56
Unigene131487	FLYFDEPDIAGHTWGPESSQIKNTIQRV DWTVGKLLGKLRKHKL	J3SEZ3	Phosphodiest	45.16
Venom auxiliary proteins				
Neprilysin-1				
CL11004.Contig1	KIVDDIRQSFRINVYNLDWMDNVAQRKT VEKVEALLAQIGYP	W4VS99	Peptidase_M13_N	33.66
CL4489.Contig2	NAYYENRVNKIVVPAGLLQPPFFHESFPN SWRFGAIGFATGHELTHGFDNNGCNYDK DGNLKNWWSNSSRKHFTARSNCIKNQY SSYTVYNEHVNGQKTLGENIADNGGIKLA HMAYHKWLRKNKGKEKTFPGISLSPEK LFFLGFAQMWCSKATLSSELSSLKTDVH SPGRVRVLGVLSNSKEFAKAFNCPKRMP MNPVKKC	W4VS99	Peptidase_M13_N	31
Unigene1677	NAFYWPPDNKIVVPTGILQPPFFSSERPRS MNYGGIGMIIGHEISHGFDTQGRLFNWD GNMVDWWTAESIRAFKNKTECFIKQYSN ISVDGLKIDGKITLSENMADNGGLKHSLK AYKKSVEKLGEEPTLPGNLGFSHEQLFFL SFAQTFCSKLTPTSLKTKLTGPHSPGRGR VIGTVSNMPEFAEAFNCRLGSNMNPKH KCS	W4VS99	Peptidase_M13_N	29.09

Table 3 (continued)

Z. natalensis contigs	Protein sequence	Uniprot match	Pfam domain	Identity (%)
Unigene12406	LIKLIEKYGSWPLGNSSWDEANWDLVKS IGIIGRDLATYPLFFFRVESERKNNTRNLI TLKQLWYFSLSKYHHLRNNTRARKVKR VFKEMMRNITVALGAVNVTDTELDDIIK FEEKLAKITVPRFRSDYYRNYQKMTLRE LNEKTGYKFDWLTFLQTMFAKTNYTVS EDEEIGVFALHYLKNLTNLLTQTPKRSIA NYVMWRVVGTKYLSLSKKFRNFYKSYA LQLYNRWSGGMVKKEECVFQLQFVSW FGMPLAKVYVDRKFSENKKNQAKKIM DDVRVAFIENLENLDWMEENSKNLAR AKAEGVIEHIGYP	W4VS99	Peptidase_M13_N	31.72
Unigene21022	NAYYSPTKNKIVFPAGILQDPFFDQNFP KSLNYGGIGMVVGHEITHGFDDNGRK FNKEGNLVKWWSNKSIENFKQKIDCL VEQYGNYSMFGKKLNGKQTLGENIAD NGGIKQSYEAYQNWVTKYGKEVPLPG LDLTHNQLFFVSFAQIWCSSWRKNSLY NQLETGVHSPGKFRVIGSLSNMAAFSE AFNCPVGSPMNKKVKCSV	W4VS99	Peptidase_M13_N	34.05
Allergen and innate immunity				
Venom dipeptidyl peptidase				
CL7419.Contig1	KAASFANSSFLIVHGSGDDNVHFQHTA QMVRKLTEAEV	B1A4F7	DPPIV_N	33.07
CL7419.Contig2	KYMRTKSYVSKDKFAIWGWSYGGFLS AYVLSKGSDLFKCAMSVAPVFSWIYYD SAYTERYMGLPQENKQGYEKTSLIDKA ASFANSSFLIVHGSGDDNVHFQHTAQM VRKLTEAEVPFRIQYYTDKAHSLWGFH TRRHLWRLLTKYLVQSV	B1A4F7	DPPIV_N	31.88

to identify the full set of venom peptides expressed by a species (Prashanth et al. 2014; Vonk et al. 2013). Although there are numerous studies on toxin diversity in cnidarians like hydra, jellyfish, and sea anemone (Li et al. 2016; Madio et al. 2017; Rachamim et al. 2015), systematic characterization of peptide toxin diversity by combining high-throughput transcriptomics and proteomics in zoantharians is practically inexistent and, until now, remained lacking in the current scientific literature.

The primary aim of this study was to identify venom-related proteins and peptide/protein toxins from a zoantharian of the genus *Zoanthus* through combined transcriptomic and proteomic analyses. A great diversity of animal toxin function has evolved from a limited number of protein families (Fry et al. 2009). Therefore, the ToxProt database was used as a strategy for the identification of potential toxins from the transcriptome of the mat anemone *Z. natalensis*. Besides, the annotated transcriptome provided a resourceful database for mass spectrometric protein identifications at the same time. To confirm the existence of the subset of these peptide/protein toxins, LC–MS/MS analysis was applied for the proteomic study. In the proteomic study, accuracy and sensitivity of peptide identification from LC–MS/MS data

directly impact the performance of protein identification from peptide hits (Ma et al. 2003). PEAKS, a de novo proteome sequencing software, could confidently identify more PSMs than Mascot and SEQUEST (Zhang et al. 2012a) and was utilized in this study, by which 64,365 PSMs were identified at a 0.5% FDR (Fig. 2).

The peptide toxins identified so far through the combination of transcriptomic and proteomic analyses were classified into six categories including neurotoxin, hemostatic and hemorrhagic toxin, protease inhibitor, mixed function enzymes, venom auxiliary proteins, and allergen and innate immunity (Fig. 3, Table 2). A total of 212 toxin-like peptides were shown to be expressed in this zoantharian mat anemone through transcriptomic deep sequencing. Meanwhile, compared with the transcriptomic results, only 30 peptide toxins were validated in the proteome. Therefore, according to his finding, most putative toxins could be expressed at very low levels or not be expressed at all in the environmental condition in which this zoanthid specimen was collected and maintained. Nematocyst proteomics was studied in other cnidarians, such as hydroids (hydras), schyphozoans (jellyfishes) and actiniarians (sea anemones), revealing, in sea anemones, ten K^+ channel toxins (KTxs),
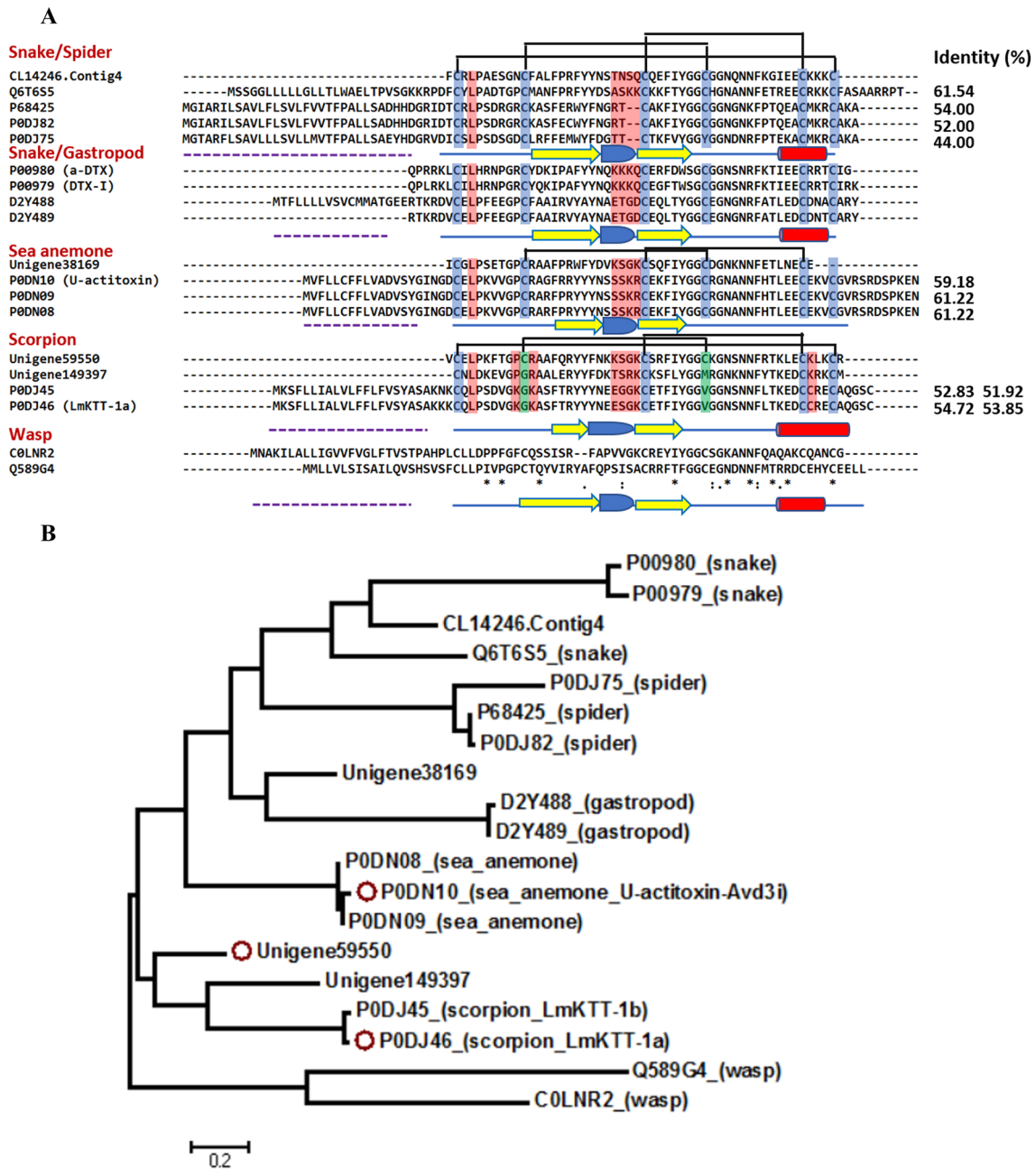
Fig. 4 Phylogenetic analysis of predicted Kunitz-like peptides from *Z. natalensis*. **a** Multiple sequence alignment of *Z. natalensis* Kunitz-like peptides and toxins originated from different species of marine and terrestrial organisms, including snake, spider, gastropod, sea anemone, scorpion, and wasp. Notably, protease inhibitor activity would decrease and only specific effect on $K_V1.3$ is maintained if cysteine residues highlighted in purple mutated to alanine. Residues highlighted in blue are cysteine and the region in red was marked as key residues which block the active sites of ion channels. The dash lines stand for signal peptide. The arrow symbols represent β-sheet, and semicircle is β-turn and cylinder, α-helix. **b** Maximum-likelihood tree of phylogenetic analysis. The *Z. natalensis* Kunitz-like peptides split in three branches through the phylogenetic relationship: snake Kunitz peptide, sea anemone Kunitz peptide, and scorpion Kunitz peptide (color figure online)

and one Na^+ channel toxin (NaTxs), while in the venoms of Aurelia (scyphozoan) and hydra cytolysins and enzymes without identifiable were the richest expressed neurotoxins (Rachamim et al. 2015). In the present study, among 30 identified peptides, five of them were neurotoxins, what indicated

that both phylogeny and toxin composition of zoantharians are concordant and shared by means of a core repertoire of peptides also seen to be expressed in sea anemones (Kayal et al. 2017).
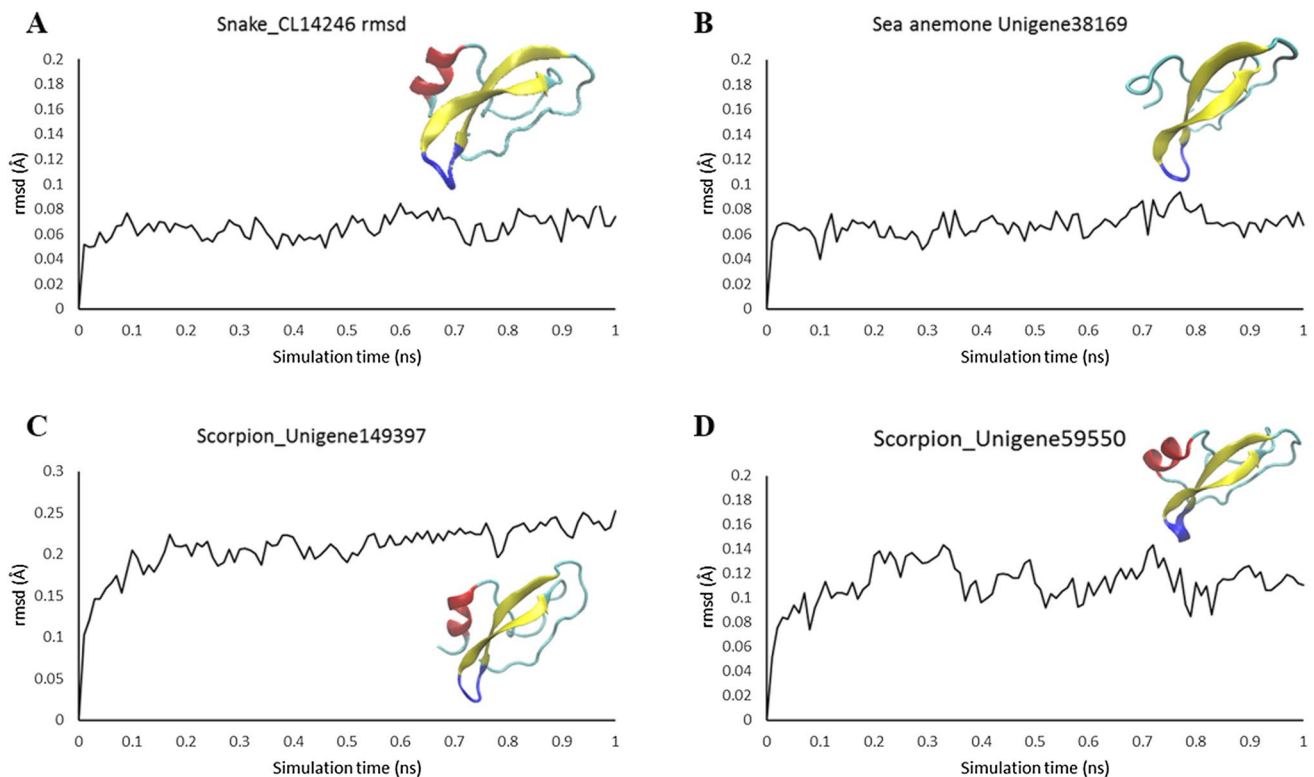
Fig. 5 Structure modeling and MD simulation of Kunitz-like peptides. Refinement was achieved by 10 ns simulation after minimization and equilibration steps. Molecule interaction was considered. The parameter "-inter" was utilized that interactively assigns charge states for Glu, Asp, Lys, Arg, and His; additionally, choosing which Cys are involved in disulfide bonds. Structures were recognized as stable when rmsd value was lower than 0.3 Å. Molecules were displayed in the Cartoon style and colored according to their secondary structure: α-helix in orange, β-sheet in yellow, and coil in cyan. The presumed binding sites are colored in blue (color figure online)

An interesting neurotoxin to investigate and expand the number of analogs for investigation on the structure–activity relationships is the members of Kunitz peptides. Multiple sequences alignment was then performed on the best matched *Z. natalensis* peptides from the transcriptomic analysis with known Kunitz peptides from snake, spider, gastropod, scorpion, wasp, and sea anemone. Kunitz peptide is a member of type II KTxs, according to the nomenclature of Cnidaria K$^+$ channel toxins that follows the proposal of Castaneda and Harvey (Castaneda and Harvey 2009). However, type II KTxs have not yet been clearly distinguished based solely on structural homology, what requires biochemical characterization (Minagawa et al. 2008). Herein, the identities of the candidate Kunitz-like peptides ranged from 40 to 60%, indicating that the *Z. natalensis* Kunitz-like peptides were conserved, presumably as a result of strong negative selection that governs the evolution of most cnidarian toxins (Jouiaei et al. 2015). Interestingly, based on the maximum-likelihood tree (Fig. 4b), Unigene59550 and Unigene149397 clustered with LmKTT-1a and LmKTT-1b, two scorpion Kunitz peptides. Within Unigene149397, only two disulfide bonds were generated because of the lack of two cysteine residues at C-terminal. The Unigene38169 was predicted

as the transcript which encodes Kunitz-like peptide based on the PFAM annotation. However, the protein sequence it expressed only contained five cysteine residues. For this scenario, the first cysteine in the sequence is flexible and reactive, which means that it may not be a stable product. Interestingly, it is possible for a peptide exist similar to this and remains biological active, such as Rattusin, an intestinal α-defensin-related peptide was composed of 31 amino acids containing five cysteines and displayed salt-insensitive antibacterial activities (Patil et al. 2013). To further investigate if this transcript exists or not, the true gene product or the peptide should be sequenced or isolated. In addition, Zhao et al. found that protease inhibitor activity of LmKTT-1a would decrease and the no change in K$_V$1.3 inhibition is observed if cysteine residues Cys72 associated with Cys80 (highlighted in purple in Fig. 4a) are mutated to Ala (Zhao et al. 2011). From the multiple sequence alignment, Lys48 of Unigene59550 matched Cys72 of LmKTT-1a, indicating that Kunitz-like peptide in *Z. natalensis* is shorter and may lack protease inhibitor activity. The oxidative folding process is shown in Fig. 7, which indicates the likeliness of its native connectivity. In most cases, such high folding yield can only be achieved when the disulfide connectivity
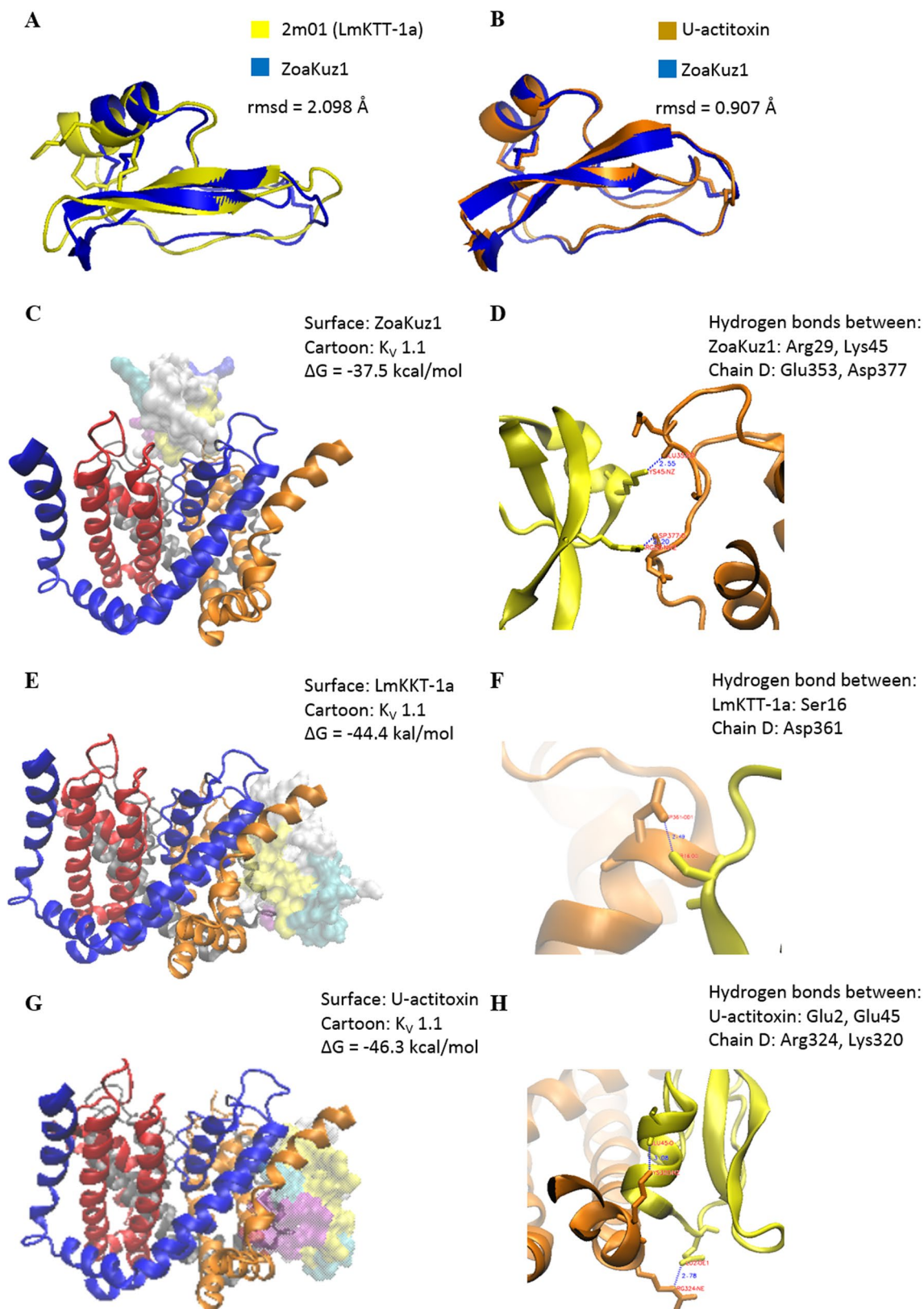
Fig. 6 Structural alignment, overlapping, and peptide–protein docking visualization. **a** Structure overlap of ZoaKuz1 and LmKTT-1a, rmsd = 2.098 Å. **b** Structure overlap of ZoaKuz1 and U-actitoxin, rmsd = 0.907 Å. Docking complex of ZoaKuz1, LmKTT-1a, and U-actitoxin with $K_V1.1$ are shown in **c**, **e**, and **g** with ΔG value of −37.5, −44.4, and −46.3 kcal/mol, whose interactive strengths are through hydrogen bonds with the bind sites shown in **d**, **f**, and **h**, respectively
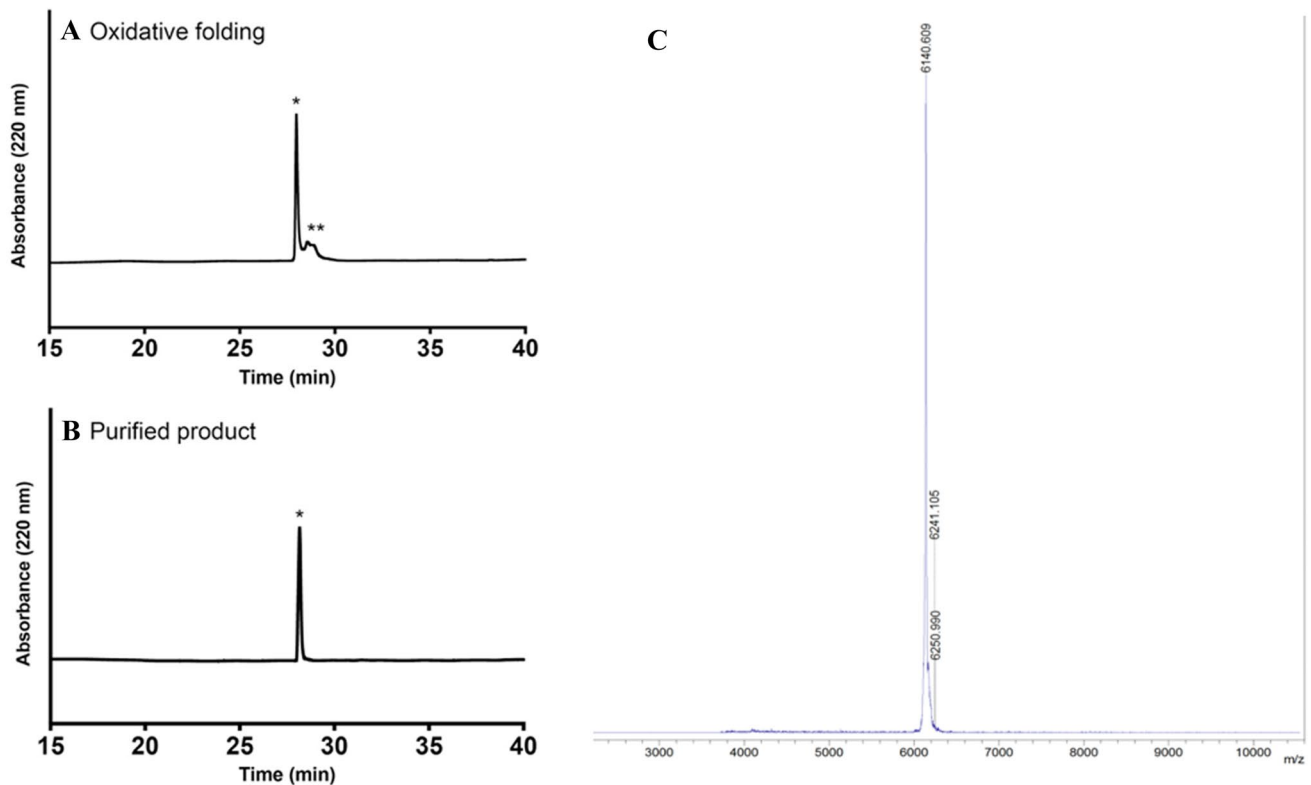
Fig. 7 RP-HPLC and MALDI-TOF profiles of the oxidative folding process of ZoaKuz1. **a** After 48 h of oxidative folding process in the presence of GSSG/GSH was monitored by RP-HPLC. Asterisk represents the correctly folded peptide, while the double asterisk represents the mixed disulfide species. **b** The purification of correctly disulfide-folded ZoaKuz1. **c** MALDI-TOF spectra of and the zoomed isotropic pattern of the purified ZoaKuz1 peptide. For $C_{271}H_{427}N_{82}O_{70}S_6$ [M+H+] 6146.85; found [M+H+] 6140.61

is native. Moreover, we previously validated the protease inhibition of PcKuz3, a Kunitz peptide from the zoantharian *Palythoa caribaeorum,* and found that the protease inhibitory was very weak (Liao et al. 2018b). In addition, the selective known Kunitz peptides from sea anemone are as long as the other Kunitz peptides families which could act both trypsin inhibitory and K$^+$ channel blockade.

Usually, Kunitz peptides could play as endogenous proteins or toxins (Rachamim et al. 2015). Kunitz peptides are vital in envenomation through serine protease inhibitory or blocking K$^+$ channel-mediated neurotransmission (Choo et al. 2012; Harvey 2001). Among the five identified neurotoxins, the expressed peptide ZoaKuz1 (Unigene59550), also identified in the shotgun proteomic sequencing, was used as template to perform peptide–protein docking analysis for investigation of its unique inhibitory mechanism against $K_V1.1$. As shown in Fig. 6, ZoaKuz1 superimposes spatially better with the known Kunitz peptide U-actitoxin-Avd3i (rmsd = 0.907 Å) than LmKTT-1a (rmsd = 2.098 Å), even though ZoaKuz1 shared higher identity with LmKTT-1a in phylogenetic analysis. It is widely known that proteins with high sequence identity and structural similarity tend to possess similar function

and evolutionary relationships, yet high sequence identity but low structure similarity can occur because of conformational plasticity, mutations, solvent effects, and ligand binding (Gan et al. 2002). Moreover, ZoaKuz1 docked well with the pore of $K_V1.1$, adopting a complex conformation, like shown in Fig. 6c, and making evident the important interactive site (Lys45) of ZoaKuz1, which is distributed within the C-terminal. In contrast, Kunitz peptides like δ-dendrotoxin and PcKuz3 mainly used the N-terminal to block $K_V1.1$ (Imredy and MacKinnon 2000; Liao et al. 2018b). Thus, ZoaKuz1 appears as a novel Kunitz-like peptide that contrasts with its counterpart in sea anemone, but that is more similar to scorpion Kunitz peptide. Importantly, scorpion toxin was reported that could process neuroprotective activity through upregulating the brain-delivery neurotrophic factor (BDNF), contributing to protect against the Aβ-induced damage (Wang et al. 2014; Zhang et al. 2016).

In this view, the present in vitro study with the disulfide bond-folded *Z. natalensis* Kunitz-like peptide elucidated that ZoaKuz1 was able to induce cytotoxicity, in PC12 cells (Figure S4). Notably, ZoaKuz1 has the ability to attenuate DA neuron loss induced by 6-OHDA in

Fig. 8 ZoaKuz1 protects against 6-OHDA-induced dopaminergic neuron loss in zebrafish. **a** Representative morphology of DA neurons in zebrafish brain indicated by immunostaining with antibody against tyrosine hydroxylase (TH). TH⁺ neurons in diencephalic region are indicated by yellow brackets. **b** Quantitative analysis of the TH⁺ neurons of each group. *Ctrl* zebrafish larvae not exposed to peptides; *Veh* vehicle, 6-OHDA-treated group. Data are expressed as a fold change normalized by control group. $^{###}p < 0.001$ versus control group, $^{***}p < 0.001$ versus 6-OHDA group (color figure online)
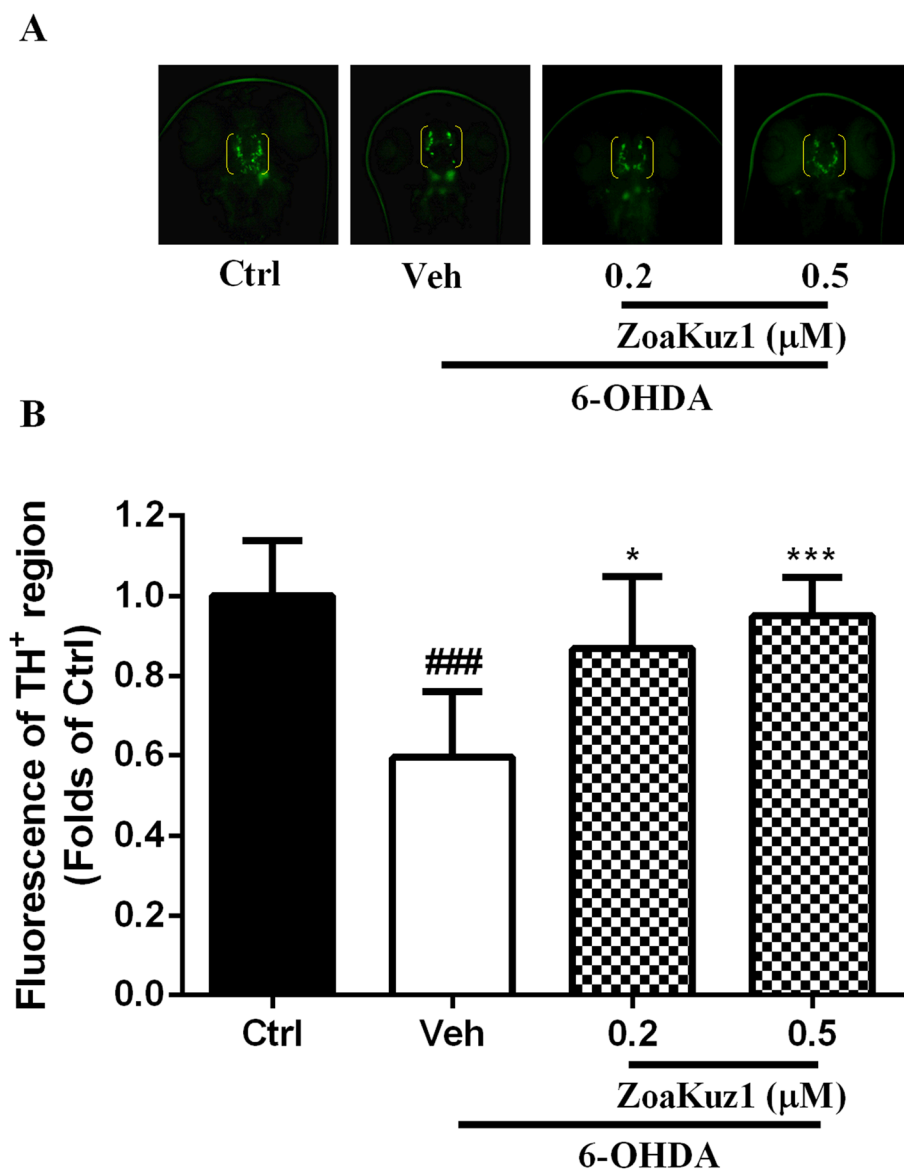
zebrafish larvae when concentration was as low as 0.5 μM (Fig. 8). Zebrafish has been considered as a suitable model for bioassay in the study due to their small size, rapid development, transparency, and developmental similarities to mammalian development (Yamashita et al. 2014). At zebrafish development stage, the larval will hatch at 3-day post-fertilization (3 dpf) (Westerfield 2000). It is accepted that the chemicals can be directly added to the water for the treatments in zebrafish embryos and larvae, which the larvae can take up the dissolved drugs through the gills (Berghmans et al. 2008; Magno et al. 2015). In this study, the zebrafish larvae were treated with ZoaKuz1 at 3 dpf. We have succeeded to access and treat the peptide contained more than 30 amino acids to zebrafish larvae by ligated a dye, rhodamine-B, at the N-terminal of the peptides, in our previous studies (Chan et al. 2017; Liao et al.

2018a). In addition, we reported that one of its Kunitz analogs, PcKuz3, could display neuroprotective effect in zebrafish larvae (Liao et al. 2018b). Although ZoKuz1 contains more than 30 amino acids, it can be absorbed by the zebrafish larvae by gills or mouth. In vivo data indicate an important neuroprotective activity of *Z. natalensis* Kuniz-type toxin, ZoaKuz1. Kunitz peptides family, HMIQ3c1 (6434 Da), from the sea anemone *Heteractis magnifica*, exhibiting neuroprotective effect, was identified by Kvetkina and collaborators that could increase cell viability of Neuro 2a cell line by $39.4 \pm 6.6\%$ in the presence of β-amyloid when concentration was at 10 μM (Kvetkina et al. 2018). We also previously reported a Kunitz-like peptide, PcKuz3, from the anthozoan *P. caribaeorum* that displayed neuroprotection by decreasing the 6-OHDA-induced lesion in zebrafish larvae (Liao et al.

Fig. 9 ZoaKuz1 reverses 6-OHDA-induced deficits in the locomotor behavior of zebrafish. **a** Representative patterns of zebrafish locomotion traced from control and treated groups. **b** Statistics analysis of total distance movement of different groups. Eight fish larvae per group from three independent experiments. $^{##}p < 0.01$ versus control group, $^{**}p < 0.01$ versus 6-OHDA group
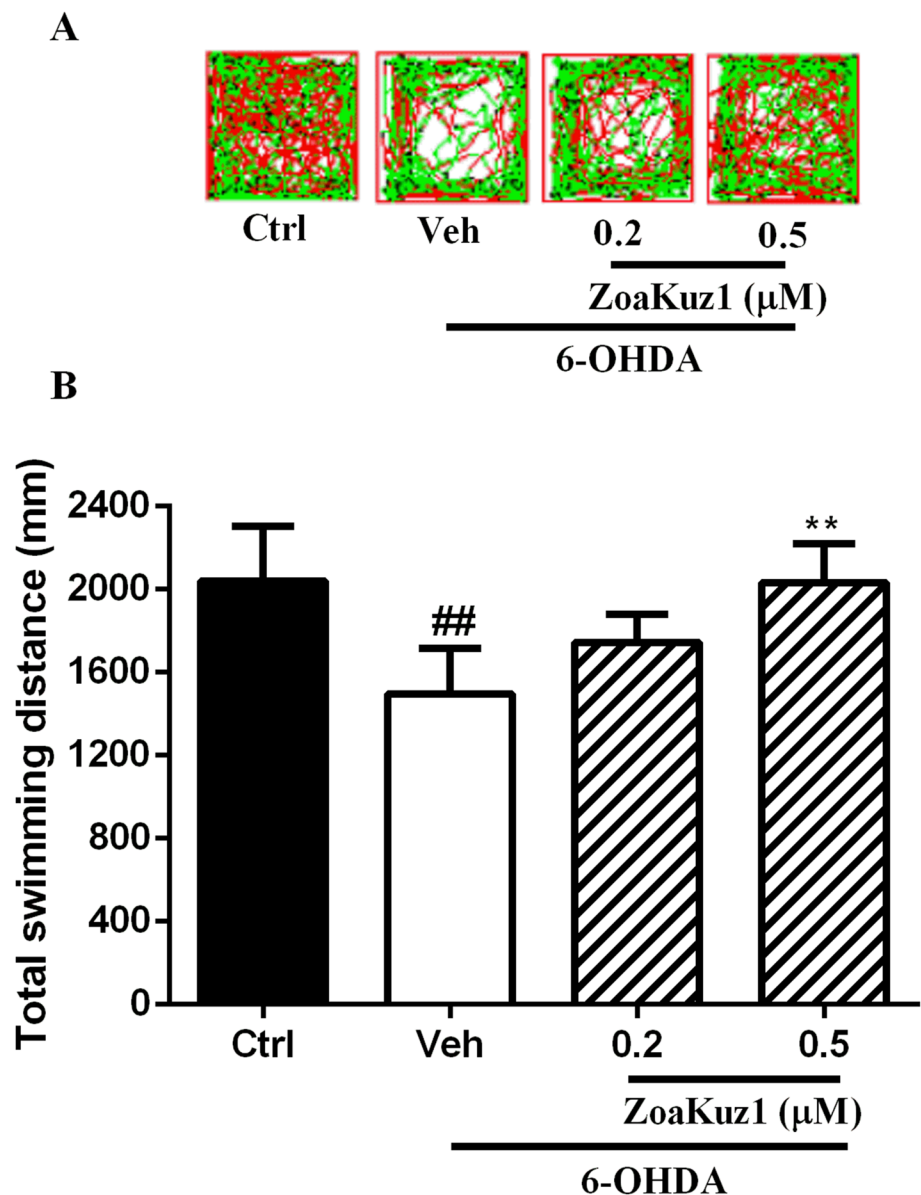
2018b). Thus, cnidarian Kunitz-like peptides highlight the potential to produce valuable therapeutic peptide leads for neuroprotection, by which the present combined transcriptomic and proteomic studies of zoanthid sea mat have contributed to reveal and expand the collection of Kunitz-containing domain analogs. In addition, our present study contributes to the cumulative evidences, demonstrating that the pharmacological blockade of K_V channels exerts significant neuroprotective effects (Reeves et al. 2016). In the same line, Fordyce and Nutile-McMnenmy proved that activated microglia could induce hippocampal neuron cell death through a process requiring microglial K_V1.3 activity and the blockade of K_V1.3 markedly diminished microglial migration to cellular debris (Fordyce et al. 2005; Nutile-McMenemy et al. 2007). Moreover, Reeves et al. discovered that both K_V1.3 and K_V1.2 were localized within axons and glia of the white matter tract after traumatic brain injury through immunohistochemistry of rat corpus callosum (Reeves et al. 2016). Koeberle and members identified K_V1.1 and K_V1.3 channels contribute to cell-autonomous death of retinal ganglion cells which K_V1.1 depletion increased anti-apoptotic gene (Bcl-X_L), whereas K_V1.3 depletion reduced the expression levels of pro-apoptotic genes (caspase-3, caspase-9, and Bad) (Koeberle et al. 2010). Again, by interacting with the pore channel, ZoaKuz1 could virtually block K_V1.1, according to our iterative docking analysis. Thus, ZoaKuz1 arises as modulator that potentially plays a vital role in neuroprotection through K_V1.1 blockade.

Last, but not least, Parkinson's disease (PD) is characterized by progressive neurodegeneration in the substantia nigra pars compacta (SNpc), affecting mainly dopaminergic neurons (Poewe et al. 2017). However, there are no disease-modifying drugs to treat PD patients, while most current treatments are symptomatic, but do not delay dopaminergic neuron degeneration (de Souza et al. 2018). In this study, ZoaKuz1 could prevent 6-OHDA-induced neuron loss in zebrafish assays. More importantly, ZoaKuz1 could attenuate 6-OHDA-induced lesion of the swimming behavior of zebrafish larvae. Thus, the structural and functional diversity of these Kunitz-type potassium channel toxins may provide an ideal approach to prevent dopaminergic neuronal cell loss in PD and, thereby, slows or even halts disease progression.

Among the K_V1 voltage-gated potassium channels, the $K_V1.1$ and $K_V1.2$ are widely represented throughout the nervous system (Kuba et al. 2015). Neurons undergoing apoptosis may lose a substantial amount of cytosolic K^+ through K^+ efflux via K_V channels (Ovsepian et al. 2016). Thus, blocking K_V channels has been shown to prevent neuronal apoptosis by preventing K^+ efflux, leading to neuroprotective effect. In this study, both $K_V1.1$ and $K_V1.2$ were selected as targets in the docking analysis. However, ZoaKuz1 could not bind to the pore region of $K_V1.2$, as shown in Figure S5, indicating that ZoKuz1 may be specific to $K_V1.1$ when acting on nervous system.

ZDOCK is used for peptide–protein analysis. The performance of ZDOCK has been demonstrated with the benchmark and worldwide blind test CAPRI, and the successful rate is about 70% with best model ranked tenth (Chen et al. 2003b). Thus, protein–protein docking was performed as the first step to investigate the potential binding site of the new Kunitz-like peptide, ZoaKuz1, and the putative interactions between protein/known ligand and protein/peptide. The docking results could provide further insight into the inhibitory process and suggest future direction to explore the molecular mechanism of action, e.g., by mutagenesis study using alanine scanning, computational mutagenesis. Based on docking results, we choose to perform in vivo assays with zebrafish model of drug screening. In the future, patch-clamp analysis is necessary to be carried out to validate the reduction of $K_V1.1$ currents impaired by ZoaKuz1.

In conclusion, to the best of our knowledge, the present study is the first to integrate de novo transcriptomic and shotgun proteomic approaches to identify the peptide toxin repertoire of *Z. natalensis*. The transcriptome has been deposited at DDBJ/EMBL/GenBank and the proteome data are available via ProteomeXchange, as aforementioned. Phylogenetic and molecular docking analysis showed that one *Z. natalensis* Kunitz-like peptide, in particular, the ZoaKuz1, is a potential K_V blocker. The functional assays, performed after chemical synthesis and successfully oxidative folding of ZoaKuz1, demonstrate that ZoaKuz1 displays

neuroprotective effect. Overall, the combined transcriptomic and proteomic study of a zoanthid revealed the expression of a cocktail of structurally diverse peptides, and demonstrated that *Z. natalensis* peptidome is a promising source of Kunitz-like peptides useful for diagnosis and adjuvant treatment of neurodegenerative disorders that are related to potassium channel dysfunction.

Compliance with ethical standards

Conflict of interest The authors declare no conflict of interest.

References

Anichtchik OV, Kaslin J, Peitsaro N, Scheinin M, Panula P (2004) Neurochemical and behavioural changes in zebrafish *Danio rerio* after systemic administration of 6-hydroxydopamine and 1-methyl-4-phenyl-1,2,3,6-tetrahydropyridine. J Neurochem 88(2):443–453

Arnold K, Bordoli L, Kopp J, Schwede T (2006) The SWISS-MODEL workspace: a web-based environment for protein structure homology modelling. Bioinformatics 22(2):195–201. https://doi.org/10.1093/bioinformatics/bti770

Balasubramanian PG, Beckmann A, Warnken U, Schnolzer M, Schuler A, Bornberg-Bauer E, Ozbek S (2012) Proteome of hydra nematocyst. J Biol Chem 287(13):9672–9681. https://doi.org/10.1074/jbc.M111.328203

Beeton C, Wulff H, Barbaria J, Clot-Faybesse O, Pennington M, Bernard D, Beraud E (2001) Selective blockade of T lymphocyte K(+) channels ameliorates experimental autoimmune encephalomyelitis, a model for multiple sclerosis. Proc Natl Acad Sci USA 98(24):13942–13947. https://doi.org/10.1073/pnas.241497298

Beeton C, Wulff H, Standifer NE, Azam P, Mullen KM, Pennington MW, Chandy KG (2006) Kv1.3 channels are a therapeutic target for T cell-mediated autoimmune diseases. Proc Natl Acad Sci USA 103(46):17414–17419. https://doi.org/10.1073/pnas.0605136103

Berghmans S, Butler P, Goldsmith P, Waldron G, Gardner I, Golder Z, Fleming A (2008) Zebrafish based assays for the assessment of cardiac, visual and gut function—potential safety screens for early drug discovery. J Pharmacol Toxicol Methods 58(1):59–68. https://doi.org/10.1016/j.vascn.2008.05.130

Castaneda O, Harvey AL (2009) Discovery and characterization of cnidarian peptide toxins that affect neuronal potassium ion channels. Toxicon 54(8):1119–1124. https://doi.org/10.1016/j.toxicon.2009.02.032

Chan JY, Zhou H, Kwan YW, Chan SW, Radis-Baptista G, Lee SM (2017) Evaluation in zebrafish model of the toxicity of rhodamine B-conjugated crotamine, a peptide potentially useful for diagnostics and therapeutics. J Biochem Mol Toxicol. https://doi.org/10.1002/jbt.21964

Chen R, Li L, Weng Z (2003a) ZDOCK: an initial-stage protein-docking algorithm. Proteins 52(1):80–87. https://doi.org/10.1002/prot.10389

Chen R, Tong W, Mintseris J, Li L, Weng Z (2003b) ZDOCK predictions for the CAPRI challenge. Proteins 52(1):68–73. https://doi.org/10.1002/prot.10388

Choo YM, Lee KS, Yoon HJ, Qiu Y, Wan H, Sohn MR, Jin BR (2012) Antifibrinolytic role of a bee venom serine protease inhibitor that acts as a plasmin inhibitor. PLoS One 7(2):e32269. https://doi.org/10.1371/journal.pone.0032269

Cruz IC, Meira VH, de Kikuchi RK, Creed JC (2016) The role of competition in the phase shift to dominance of the zoanthid Palythoa cf. variabilis on coral reefs. Mar Environ Res 115:28–35. https://doi.org/10.1016/j.marenvres.2016.01.008

de Souza JM, Goncalves BDC, Gomez MV, Vieira LB, Ribeiro FM (2018) Animal toxins as therapeutic tools to treat neurodegenerative diseases. Front Pharmacol 9:145. https://doi.org/10.3389/fphar.2018.00145

Deutsch EW, Csordas A, Sun Z, Jarnuczak A, Perez-Riverol Y, Ternent T, Vizcaino JA (2017) The ProteomeXchange consortium in 2017: supporting the cultural change in proteomics public data deposition. Nucleic Acids Res 45(D1):D1100–D1106. https://doi.org/10.1093/nar/gkw936

Diochot S, Baron A, Rash LD, Deval E, Escoubas P, Scarzello S, Lazdunski M (2004) A new sea anemone peptide, APETx2, inhibits ASIC3, a major acid-sensitive channel in sensory neurons. EMBO J 23(7):1516–1525. https://doi.org/10.1038/sj.emboj.7600177

Edgar RC (2004) MUSCLE: multiple sequence alignment with high accuracy and high throughput. Nucleic Acids Res 32(5):1792–1797. https://doi.org/10.1093/nar/gkh340

Erwin DH, Laflamme M, Tweedt SM, Sperling EA, Pisani D, Peterson KJ (2011) The Cambrian conundrum: early divergence and later ecological success in the early history of animals. Science 334(6059):1091–1097. https://doi.org/10.1126/science.1206375

FastQC: a quality control tool for high throughput sequence data (2011). https://www.bioinformatics.babraham.ac.uk/projects/fastqc/. Accessed 1 Apr 2017

Fordyce CB, Jagasia R, Zhu X, Schlichter LC (2005) Microglia Kv1.3 channels contribute to their ability to kill neurons. J Neurosci 25(31):7139–7149. https://doi.org/10.1523/jneurosci.1251-05.2005

Fry BG, Roelants K, Champagne DE, Scheib H, Tyndall JD, King GF, de la Vega RC (2009) The toxicogenomic multiverse: convergent recruitment of proteins into animal venoms. Annu Rev Genom Hum Genet 10:483–511. https://doi.org/10.1146/annurev.genom.9.081307.164356

Gan HH, Perlow RA, Roy S, Ko J, Wu M, Huang J, Schlick T (2002) Analysis of protein sequence/structure similarity relationships. Biophys J 83(5):2781–2791

Haas BJ, Papanicolaou A, Yassour M, Grabherr M, Blood PD, Bowden J, Regev A (2013) De novo transcript sequence reconstruction from RNA-seq using the Trinity platform for reference generation and analysis. Nat Protoc 8(8):1494–1512. https://doi.org/10.1038/nprot.2013.084

Harvey AL (2001) Twenty years of dendrotoxins. Toxicon 39(1):15–26

Huang C, Morlighem JR, Zhou H, Lima EP, Gomes PB, Cai J, Radis-Baptista G (2016) The transcriptome of the Zoanthid Protopalythoa variabilis (Cnidaria, Anthozoa) predicts a basal repertoire of toxin-like and venom-auxiliary polypeptides. Genome Biol Evol 8(9):3045–3064. https://doi.org/10.1093/gbe/evw204

Humphrey W, Dalke A, Schulten K (1996) VMD: visual molecular dynamics. J Mol Graph 14(1):33–38

Imredy JP, MacKinnon R (2000) Energetic and structural interactions between delta-dendrotoxin and a voltage-gated potassium channel. J Mol Biol 296(5):1283–1294. https://doi.org/10.1006/jmbi.2000.3522

Jensen JE, Cristofori-Armstrong B, Anangi R, Rosengren KJ, Lau CH, Mobli M, Rash LD (2014) Understanding the molecular basis of toxin promiscuity: the analgesic sea anemone peptide APETx2 interacts with acid-sensing ion channel 3 and hERG channels via overlapping pharmacophores. J Med Chem 57(21):9195–9203. https://doi.org/10.1021/jm501400p

Jouiaei M, Sunagar K, Federman Gross A, Scheib H, Alewood PF, Moran Y, Fry BG (2015) Evolution of an ancient venom: recognition of a novel family of cnidarian toxins and the common evolutionary origin of sodium and potassium neurotoxins in sea anemone. Mol Biol Evol 32(6):1598–1610. https://doi.org/10.1093/molbev/msv050

Jungo F, Bougueleret L, Xenarios I, Poux S (2012) The UniProtKB/Swiss-Prot Tox-Prot program: a central hub of integrated venom protein data. Toxicon 60(4):551–557. https://doi.org/10.1016/j.toxicon.2012.03.010

Kayal E, Bastian B, Pankey MS, Ohdera A, Medina M, Plachetzki DC, Ryan JF (2017) Comprehensive phylogenomic analyses resolve cnidarian relationships and the origins of key organismal traits. PeerJ Prepr 5:e3172v1. https://doi.org/10.7287/peerj.preprints.3172v1

King GF (2011) Venoms as a platform for human drugs: translating toxins into therapeutics. Expert Opin Biol Ther 11(11):1469–1484. https://doi.org/10.1517/14712598.2011.621940

Koeberle PD, Wang Y, Schlichter LC (2010) Kv1.1 and Kv1.3 channels contribute to the degeneration of retinal ganglion cells after optic nerve transection in vivo. Cell Death Differ 17(1):134–144. https://doi.org/10.1038/cdd.2009.113

Kuba H, Yamada R, Ishiguro G, Adachi R (2015) Redistribution of Kv1 and Kv7 enhances neuronal excitability during structural axon initial segment plasticity. Nat Commun 6:8815. https://doi.org/10.1038/ncomms9815

Kvetkina A, Leychenko E, Yurchenko E, Pislyagin E, Peigneur S, Tytgat Y, Kozlovskaya E (2018) A new Iq-peptide of the Kunitz type from the *Heteractis magnifica* sea anemone exhibits neuroprotective activity in a model of Alzheimer's disease. Russ J Bioorg Chem 44(4):416–423

Lazcano-Perez F, Hernandez-Guzman U, Sanchez-Rodriguez J, Arreguin-Espinosa R (2016) Cnidarian neurotoxic peptides affecting central nervous system targets. Cent Nerv Syst Agents Med Chem 16(3):173–182

Lazcano-Perez F, Zavala-Moreno A, Rufino-Gonzalez Y, Ponce-Macotela M, Garcia-Arredondo A, Cuevas-Cruz M, Arreguin-Espinosa R (2018) Hemolytic, anticancer and antigiardial activity of *Palythoa caribaeorum* venom. J Venom Anim Toxins Incl Trop Dis 24:12. https://doi.org/10.1186/s40409-018-0149-8

Li H, Durbin R (2010) Fast and accurate long-read alignment with Burrows–Wheeler transform. Bioinformatics 26(5):589–595. https://doi.org/10.1093/bioinformatics/btp698

Li H, Handsaker B, Wysoker A, Fennell T, Ruan J, Homer N, Genome Project Data Processing, S (2009) The sequence alignment/map format and SAMtools. Bioinformatics 25(16):2078–2079. https://doi.org/10.1093/bioinformatics/btp352

Li R, Yu H, Yue Y, Liu S, Xing R, Chen X, Li P (2016) Combined proteomics and transcriptomics identifies sting-related toxins of jellyfish *Cyanea nozakii*. J Proteom 148:57–64. https://doi.org/10.1016/j.jprot.2016.07.023

Liao Q, Gong G, Siu SWI, Wong CTT, Yu H, Tse YC, Lee SM (2018a) A novel ShK-like toxic peptide from the transcriptome of the Cnidarian *Palythoa caribaeorum* displays neuroprotection and cardioprotection in zebrafish. Toxins (Basel). https://doi.org/10.3390/toxins10060238

Liao Q, Li S, Siu SWI, Yang B, Huang C, Chan JY, Lee SM (2018b) Novel Kunitz-like peptides discovered in the Zoanthid *Palythoa caribaeorum* through transcriptome sequencing. J Proteome Res 17(2):891–902. https://doi.org/10.1021/acs.jproteome.7b00686

Ma B, Zhang K, Hendrie C, Liang C, Li M, Doherty-Kirby A, Lajoie G (2003) PEAKS: powerful software for peptide de novo sequencing by tandem mass spectrometry. Rapid Commun Mass Spectrom 17(20):2337–2342. https://doi.org/10.1002/rcm.1196

Macrander J, Brugler MR, Daly M (2015) A RNA-seq approach to identify putative toxins from acrorhagi in aggressive and non-aggressive *Anthopleura elegantissima* polyps. BMC Genom 16:221. https://doi.org/10.1186/s12864-015-1417-4

Madio B, Undheim EAB, King GF (2017) Revisiting venom of the sea anemone *Stichodactyla haddoni*: omics techniques reveal the complete toxin arsenal of a well-studied sea anemone genus. J Proteom 166:83–92. https://doi.org/10.1016/j.jprot.2017.07.007

Magno LD, Fontes A, Goncalves BM, Gouveia A Jr (2015) Pharmacological study of the light/dark preference test in zebrafish (*Danio rerio*): waterborne administration. Pharmacol Biochem Behav 135:169–176. https://doi.org/10.1016/j.pbb.2015.05.014

Michalski A, Damoc E, Hauschild JP, Lange O, Wieghaus A, Makarov A, Horning S (2011) Mass spectrometry-based proteomics using Q Exactive, a high-performance benchtop quadrupole Orbitrap mass spectrometer. Mol Cell Proteom 10(9):M111-011015. https://doi.org/10.1074/mcp.m111.011015

Minagawa S, Sugiyama M, Ishida M, Nagashima Y, Shiomi K (2008) Kunitz-type protease inhibitors from acrorhagi of three species of sea anemones. Comp Biochem Physiol B Biochem Mol Biol 150(2):240–245. https://doi.org/10.1016/j.cbpb.2008.03.010

Moreels L, Peigneur S, Galan DT, De Pauw E, Beress L, Waelkens E, Tytgat J (2017) APETx4, a novel sea anemone toxin and a modulator of the cancer-relevant potassium channel KV10.1. Mar Drugs. https://doi.org/10.3390/md15090287

Nutile-McMenemy N, Elfenbein A, Deleo JA (2007) Minocycline decreases in vitro microglial motility, beta1-integrin, and Kv1.3 channel expression. J Neurochem 103(5):2035–2046. https://doi.org/10.1111/j.1471-4159.2007.04889.x

Oldrati V, Arrell M, Violette A, Perret F, Sprungli X, Wolfender JL, Stocklin R (2016) Advances in venomics. Mol Biosyst 12(12):3530–3543. https://doi.org/10.1039/c6mb00516k

Ovsepian SV, LeBerre M, Steuber V, O'Leary VB, Leibold C, Oliver Dolly J (2016) Distinctive role of KV1.1 subunit in the biology and functions of low threshold K(+) channels with implications for neurological disease. Pharmacol Ther 159:93–101. https://doi.org/10.1016/j.pharmthera.2016.01.005

Ozbek S, Balasubramanian PG, Holstein TW (2009) Cnidocyst structure and the biomechanics of discharge. Toxicon 54(8):1038–1045. https://doi.org/10.1016/j.toxicon.2009.03.006

Park E, Hwang DS, Lee JS, Song JI, Seo TK, Won YJ (2012) Estimation of divergence times in cnidarian evolution based on mitochondrial protein-coding genes and the fossil record. Mol Phylogenet Evol 62(1):329–345. https://doi.org/10.1016/j.ympev.2011.10.008

Patil AA, Ouellette AJ, Lu W, Zhang G (2013) Rattusin, an intestinal alpha-defensin-related peptide in rats with a unique cysteine spacing pattern and salt-insensitive antibacterial activities. Antimicrob Agents Chemother 57(4):1823–1831. https://doi.org/10.1128/AAC.02237-12

Peigneur S, Tytgat J (2018) Toxins in drug discovery and pharmacology. Toxins (Basel). https://doi.org/10.3390/toxins10030126

Perez-Riverol Y, Xu QW, Wang R, Uszkoreit J, Griss J, Sanchez A, Vizcaino JA (2016) PRIDE inspector toolsuite: moving toward a universal visualization tool for proteomics data standard formats and quality assessment of proteomeXchange datasets. Mol Cell Proteom 15(1):305–317. https://doi.org/10.1074/mcp.O115.050229

Pertea G, Huang X, Liang F, Antonescu V, Sultana R, Karamycheva S, Quackenbush J (2003) TIGR gene indices clustering tools (TGICL): a software system for fast clustering of large EST datasets. Bioinformatics 19(5):651–652

Pierce BG, Hourai Y, Weng Z (2011) Accelerating protein docking in ZDOCK using an advanced 3D convolution library. PLoS One 6(9):e24657. https://doi.org/10.1371/journal.pone.0024657

Poewe W, Seppi K, Tanner CM, Halliday GM, Brundin P, Volkmann J, Lang AE (2017) Parkinson disease. Nat Rev Dis Prim 3:17013. https://doi.org/10.1038/nrdp.2017.13

Prashanth JR, Lewis RJ, Dutertre S (2012) Towards an integrated venomics approach for accelerated conopeptide discovery. Toxicon 60(4):470–477. https://doi.org/10.1016/j.toxicon.2012.04.340

Prashanth JR, Brust A, Jin AH, Alewood PF, Dutertre S, Lewis RJ (2014) Cone snail venomics: from novel biology to novel therapeutics. Future Med Chem 6(15):1659–1675. https://doi.org/10.4155/fmc.14.99

Prashanth JR, Hasaballah N, Vetter I (2017) Pharmacological screening technologies for venom peptide discovery. Neuropharmacology 127:4–19. https://doi.org/10.1016/j.neuropharm.2017.03.038

Prentis PJ, Pavasovic A, Norton RS (2018) Sea anemones: quiet achievers in the field of peptide toxins. Toxins (Basel). https://doi.org/10.3390/toxins10010036

Pronk S, Pall S, Schulz R, Larsson P, Bjelkmar P, Apostolov R, Lindahl E (2013) GROMACS 4.5: a high-throughput and highly parallel open source molecular simulation toolkit. Bioinformatics 29(7):845–854. https://doi.org/10.1093/bioinformatics/btt055

Quinlan AR, Hall IM (2010) BEDTools: a flexible suite of utilities for comparing genomic features. Bioinformatics 26(6):841–842. https://doi.org/10.1093/bioinformatics/btq033

Rachamim T, Morgenstern D, Aharonovich D, Brekhman V, Lotan T, Sher D (2015) The dynamically evolving nematocyst content of an anthozoan, a scyphozoan, and a hydrozoan. Mol Biol Evol 32(3):740–753. https://doi.org/10.1093/molbev/msu335

Reeves TM, Trimmer PA, Colley BS, Phillips LL (2016) Targeting Kv1.3 channels to reduce white matter pathology after traumatic brain injury. Exp Neurol 283(Pt A):188–203. https://doi.org/10.1016/j.expneurol.2016.06.011

Reimer NS, Yasunobu CL, Yasunobu KT, Norton TR (1985) Amino acid sequence of the *Anthopleura xanthogrammica* heart stimulant, anthopleurin-B. J Biol Chem 260(15):8690–8693

Reimer JD, Ono S, Takishita K, Tsukahara J, Maruyama T (2006) Molecular evidence suggesting species in the zoanthid genera Palythoa and Protopalythoa (Anthozoa: Hexacorallia) are congeneric. Zool Sci 23(1):87–94. https://doi.org/10.2108/zsj.23.87

Reimer JD, Takishita K, Ono S, Tsukahara J, Maruyama T (2007) Molecular evidence suggesting interspecific hybridization in Zoanthus spp. (Anthozoa: Hexacorallia). Zool Sci 24(4):346–359. https://doi.org/10.2108/zsj.24.346

Reimer JD, Poliseno A, Hoeksema BW (2014) Shallow-water zoantharians (Cnidaria, Hexacorallia) from the Central Indo-Pacific. Zookeys 444:1–57. https://doi.org/10.3897/zookeys.444.7537

Robinson SD, Undheim EAB, Ueberheide B, King GF (2017) Venom peptides as therapeutics: advances, challenges and the future of venom-peptide discovery. Expert Rev Proteom 14(10):931–939. https://doi.org/10.1080/14789450.2017.1377613

Schneider CA, Rasband WS, Eliceiri KW (2012) NIH Image to ImageJ: 25 years of image analysis. Nat Methods 9(7):671–675

Tamura K, Stecher G, Peterson D, Filipski A, Kumar S (2013) MEGA6: molecular evolutionary genetics analysis version 6.0. Mol Biol Evol 30(12):2725–2729. https://doi.org/10.1093/molbev/mst197

Tarcha EJ, Olsen CM, Probst P, Peckham D, Munoz-Elias EJ, Kruger JG, Iadonato SP (2017) Safety and pharmacodynamics of

dalazatide, a Kv1.3 channel inhibitor, in the treatment of plaque psoriasis: a randomized phase 1b trial. PLoS One 12(7):e0180762. https://doi.org/10.1371/journal.pone.0180762

UniProt Consortium, T (2018) UniProt: the universal protein knowledgebase. Nucleic Acids Res 46(5):2699. https://doi.org/10.1093/nar/gky092

Van Der Spoel D, Lindahl E, Hess B, Groenhof G, Mark AE, Berendsen HJ (2005) GROMACS: fast, flexible, and free. J Comput Chem 26(16):1701–1718. https://doi.org/10.1002/jcc.20291

Vizcaino JA, Deutsch EW, Wang R, Csordas A, Reisinger F, Rios D, Hermjakob H (2014) ProteomeXchange provides globally coordinated proteomics data submission and dissemination. Nat Biotechnol 32(3):223–226. https://doi.org/10.1038/nbt.2839

Vizcaino JA, Csordas A, del-Toro N, Dianes JA, Griss J, Lavidas I, Hermjakob H (2016) 2016 update of the PRIDE database and its related tools. Nucleic Acids Res 44(D1):D447–D456. https://doi.org/10.1093/nar/gkv1145

Vonk FJ, Casewell NR, Henkel CV, Heimberg AM, Jansen HJ, McCleary RJ, Richardson MK (2013) The king cobra genome reveals dynamic gene evolution and adaptation in the snake venom system. Proc Natl Acad Sci USA 110(51):20651–20656. https://doi.org/10.1073/pnas.1314702110

Wang T, Wang SW, Zhang Y, Wu XF, Peng Y, Cao Z, Zhao J (2014) Scorpion venom heat-resistant peptide (SVHRP) enhances neurogenesis and neurite outgrowth of immature neurons in adult mice by up-regulating brain-derived neurotrophic factor (BDNF). PLoS One 9(10):e109977. https://doi.org/10.1371/journal.pone.0109977

Westerfield M (2000) A guide for the laboratory use of zebrafish (Danio rerio) Eugene, 4th edn. University of Oregon Press, pp 1.1, 9.7, 10.16

Weston AJ, Dunlap WC, Shick JM, Klueter A, Iglic K, Vukelic A, Long PF (2012) A profile of an endosymbiont-enriched fraction of the coral Stylophora pistillata reveals proteins relevant to microbial–host interactions. Mol Cell Proteom 11(6):M111-015487. https://doi.org/10.1074/mcp.m111.015487

Wisniewski JR, Mann M (2012) Consecutive proteolytic digestion in an enzyme reactor increases depth of proteomic and phosphoproteomic analysis. Anal Chem 84(6):2631–2637. https://doi.org/10.1021/ac300006b

Wisniewski JR, Zougman A, Nagaraj N, Mann M (2009) Universal sample preparation method for proteome analysis. Nat Methods 6(5):359–362. https://doi.org/10.1038/nmeth.1322

Yamashita A, Inada H, Chihara K, Yamada T, Deguchi J, Funabashi H (2014) Improvement of the evaluation method for teratogenicity using zebrafish embryos. J Toxicol Sci 39(3):453–464

Young GA, Hagadorn JW (2010) The fossil record of cnidarian medusae. Palaeoworld 19(3):212–221. https://doi.org/10.1016/j.palwor.2010.09.014

Zhang J, Xin L, Shan B, Chen W, Xie M, Yuen D, Ma B (2012a) PEAKS DB: de novo sequencing assisted database search for sensitive and accurate peptide identification. Mol Cell Proteom 11(4):M111-010587. https://doi.org/10.1074/mcp.m111.010587

Zhang ZJ, Cheang LC, Wang MW, Li GH, Chu IK, Lin ZX, Lee SM (2012b) Ethanolic extract of fructus Alpinia oxyphylla protects against 6-hydroxydopamine-induced damage of PC12 cells in vitro and dopaminergic neurons in zebrafish. Cell Mol Neurobiol 32(1):27–40. https://doi.org/10.1007/s10571-011-9731-0

Zhang XG, Wang X, Zhou TT, Wu XF, Peng Y, Zhang WQ, Zhao J (2016) Scorpion venom heat-resistant peptide protects transgenic Caenorhabditis elegans from beta-amyloid toxicity. Front Pharmacol 7:227. https://doi.org/10.3389/fphar.2016.00227

Zhao R, Dai H, Qiu S, Li T, He Y, Ma Y, Cao Z (2011) SdPI, the first functionally characterized Kunitz-type trypsin inhibitor from scorpion venom. PLoS One 6(11):e27548. https://doi.org/10.1371/journal.pone.0027548

Zhao F, Lan X, Li T, Xiang Y, Zhao F, Zhang Y, Lee WH (2018) Proteotranscriptomic analysis and discovery of the profile and diversity of toxin-like proteins in centipede. Mol Cell Proteom 17(4):709–720. https://doi.org/10.1074/mcp.RA117.000431